FINITE ELEMENT SOLUTION OF THE INTERACTION OF A PLANE ACOUSTIC BLAST WAVE AND A CYLINDRIC STRUCTURE
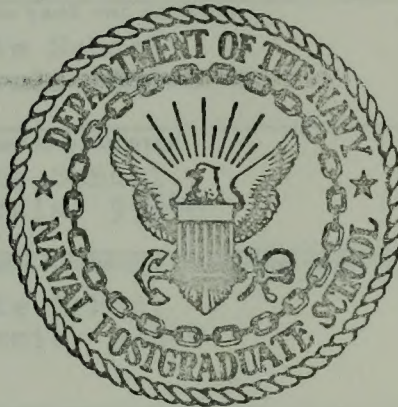
Donald Lee Atchison

NAVAL POSTGRADUATE SCHOOL
Monterey, California

THESIS

FINITE ELEMENT SOLUTION OF THE INTERACTION
OF A PLANE ACOUSTIC BLAST WAVE
AND A CYLINDRIC STRUCTURE

by

Donald Lee Atchison

June 1974

Thesis Advisor: R.E. Newton

T161728

REPORT DOCUMENTATION PAGE		READ INSTRUCTIONS BEFORE COMPLETING FORM
1. REPORT NUMBER	2. GOVT ACCESSION NO.	3. RECIPIENT'S CATALOG NUMBER
4. TITLE (and Subtitle) Finite Element Solution of the Interaction of a Plane Acoustic Blast Wave and a Cylindric Structure		5. TYPE OF REPORT & PERIOD COVERED Engineer's Thesis; June 1974
		6. PERFORMING ORG. REPORT NUMBER
7. AUTHOR(s) Donald Lee Atchison		8. CONTRACT OR GRANT NUMBER(s)
9. PERFORMING ORGANIZATION NAME AND ADDRESS Naval Postgraduate School Monterey, California 93940		10. PROGRAM ELEMENT, PROJECT, TASK AREA & WORK UNIT NUMBERS
11. CONTROLLING OFFICE NAME AND ADDRESS Naval Postgraduate School Monterey, California 93940		12. REPORT DATE June 1974
		13. NUMBER OF PAGES 80
14. MONITORING AGENCY NAME & ADDRESS(If different from Controlling Office) Naval Postgraduate School Monterey, California 93940		15. SECURITY CLASS. (of this report) Unclassified
		15a. DECLASSIFICATION/DOWNGRADING SCHEDULE

16. DISTRIBUTION STATEMENT (of this Report)

Approved for public release; distribution unlimited.

17. DISTRIBUTION STATEMENT (of the abstract entered in Block 20, if different from Report)

18. SUPPLEMENTARY NOTES

19. KEY WORDS (Continue on reverse side if necessary and identify by block number)

Finite Element
Blast Wave Propagation
Cylindrical Structure
Transient Fluid-Structure Interaction
Elasto-Hydrodynamic System

20. ABSTRACT (Continue on reverse side if necessary and identify by block number)

The finite element method is used to study the structural response of a submarine to an acoustic blast wave. Encounter geometry is restricted to the case of a plane wave front parallel to the axis of a right-circular cylindric structure. It is shown that the blast wave propagation may be studied separately from the structural response. For the case considered this separation allows a two-dimensional formulation

DD FORM 1473 EDITION OF 1 NOV 65 IS OBSOLETE
1 JAN 73
(Page 1) S/N 0102-014-6601 |

2

(20. ABSTRACT continued)

of the propagation problem while retaining a three-dimensional structural model. Propagation results are found to agree well with analytic results obtained by others.

Finite Element Solution of the Interaction
of a Plane Acoustic Blast Wave
and a Cylindric Structure

by

Donald Lee Atchison
Lieutenant, United States Navy
B.S.M.E., Purdue University, 1968

Submitted in partial fulfillment of the
requirements for the degrees of

MECHANICAL ENGINEER

and

MASTER OF SCIENCE IN MECHANICAL ENGINEERING

from the

NAVAL POSTGRADUATE SCHOOL
June 1974

Thesis
A85
c.1

ABSTRACT

The finite element method is used to study the structural response of a submarine to an acoustic blast wave. Encounter geometry is restricted to the case of a plane wave front parallel to the axis of a right-circular cylindric structure It is shown that the blast wave propagation may be studied separately from the structural response. For the case considered this separation allows a two-dimensional formulation of the propagation problem while retaining a three-dimensional structural model. Propagation results are found to agree well with analytic results obtained by others.

TABLE OF CONTENTS

LIST OF TABLES

LIST OF FIGURES

ACKNOWLEDGEMENT

The author wishes to express his appreciation to
Dr. Robert E. Newton, Professor of Mechanical Engineering,
for his advice and guidance during the course of this
investigation. Without his personal involvement and patience
this investigation could not have been completed in its
present form.

The author is also obliged to Dr. Gilles Cantin,
Professor of Mechanical Engineering, for providing two
computer subroutines used to solve large systems of equations.
Thanks are also extended to the staff of the W. R. Church
Computer Center of the Naval Postgraduate School.

Finally the author thanks his wife, Judy, for her
patience and understanding throughout his work at this
institution.

I. <u>INTRODUCTION</u>

Consider a nonrigid structure submerged in a fluid. Pressure in the fluid may induce response motions of the structure. Conversely, motion of the structure affects the pressure field. Such a system is called a coupled elasto-hydrodynamic system.

Many practical engineering problems belong to this category. A reservoir-dam system subjected to earthquake motion, oscillations in rocket fuel systems, a vibrating ship's hull, and structures subjected to blast loadings due to explosions are familiar elasto-hydrodynamic problems.

The particular elasto-hydrodynamic system under consideration in this paper is a submarine subjected to a blast wave resulting from an underwater explosion. The submarine is modeled as a ring-reinforced, neutrally buoyant, circular cylinder with rigid bulkheads. It is assumed that the blast wave may be modeled as a plane acoustic wave with wave-front parallel to the longitudinal axis of the submarine.

The interaction of an acoustic wave with an obstacle has been the subject of many investigations. Sette [1] first computed the pressure distribution on a rigid cylindrical surface due to a step-pulse. The response of a cylindrical shell to a plane step (or decaying) shock wave has been treated by various authors [2-5].

Due to the complex nature of the coupled response a realistic analytic formulation of this problem is intractable.

However, numerical methods, particularly the finite element method, provide a satisfactory means of solution.

The finite element formulation of structure-fluid dynamics was first introduced by Zienkiewicz, Irons and Nath [6]. They demonstrated that the coupled natural frequencies and mode shapes of systems could be accurately determined by this method.

It is the purpose of this paper to demonstrate that the finite element method, as forwarded by Zienkiewicz and Newton [7], is applicable to the solution of the interaction of a blast wave with a rigid structure. Using the finite element formulation, a superposition theorem is developed which affords a method of applying the rigid cylinder results to a realistic, but simple, three-dimensional model of the submarine.

II. THE FINITE ELEMENT METHOD OF SOLUTION

A. THE STRUCTURE DISCRETIZATION

The finite element discretization of the structure
problem is well known and is described in Zienkiewicz's
text [8]. The discretization process results in an
assembled system of equations of the form

$$[M]\{\ddot{\delta}\} + [C]\{\dot{\delta}\} + [K]\{\delta\} = \{R\} \quad . \qquad (1)$$

In the above equation $[M]$, $[C]$ and $[K]$ are respectively the
mass, damping, and stiffness matrices of the structure
calculated in the proper, consistent, manner, $\{\delta\}$ is a vector
of nodal displacements, the dots indicate time differentiation,
and $\{R\}$ is a vector of generalized nodal loads.

It is convenient to divide the generalized nodal forces
into two parts (after Zienkiewicz and Newton [7]) such that

$$\{R\} = \{F\} + \{P\} \quad . \qquad (2)$$

The vector $\{F\}$ is due to external forces and $\{P\}$ is due to
the fluid pressure on the interface. For the ith structural
node

$$P_i = \int_S N_i' \ p \ dS \quad , \qquad (3)$$

where N_i' is the appropriate shape function defining the
displacement pattern in the direction normal to the boundary,

13

p is the pressure on the structure-fluid interface S, and
the integration is over the interface.

B.   THE FLUID DISCRETIZATION

From first principles it can be shown [6,9] that the
wave equation

$$\nabla^2 \dot{p} = \frac{1}{c^2} \dddot{p} \quad ,$$
(4)

where ∇^2 is the Laplace operator, p is the hydrodynamic
pressure in excess of static pressure and c the acoustic
velocity of propagation, together with the necessary
boundary and initial conditions are the governing relations
for the hydrodynamic response of the fluid.

The spatial discretization of the fluid problem is
accomplished by a direct application of the Galerkin weighted
residual process. If at any instant of time p is approximated
by

$$p = N_j p_j \qquad \text{(summation on } j = 1,\ldots,m) \quad ,$$
(5)

where m is the number of nodes, N_j the jth shape function
chosen to describe the spatial variation of p over the region
and p_j is a set of nodal pressure values which are time
dependent, then the ith weighted residual equation is

$$\int_R N_i [\nabla^2 (N_j p_j) - \frac{1}{c^2} (N_j \ddot{p}_j)] \, dR = 0 \quad ,$$
(6)

where N_i is the shape (weighting) function [8, Ch. 3] of the Galerkin process and R is the fluid region under consideration. Employing Green's theorem, the weighted residual equations may be transformed to

$$\int_R [\frac{\partial N_i}{\partial x} \frac{\partial N_j}{\partial x} + \frac{\partial N_i}{\partial y} \frac{\partial N_j}{\partial y} + \frac{\partial N_i}{\partial z} \frac{\partial N_j}{\partial z}] \, dR \, p_j$$

$$+ \frac{1}{c^2} \int_R N_i N_j \, dR \, \ddot{p}_j - \int_S N_i \frac{\partial N_j}{\partial n} \, dS \, p_j = 0 . \tag{7}$$

This system of equations can be written in matrix form as

$$[Q]\{\ddot{p}\} + [H]\{p\} = \{B\} . \tag{8}$$

The matrices [Q] and [H] are the assembled "inertia" and "stiffness" matrices of the fluid. They are defined on the element level by:

$$q_{ij} = \frac{1}{c^2} \int_{R_e} N_i N_j \, dR_e , \tag{9}$$

$$h_{ij} = \int_{R_e} [\frac{\partial N_i}{\partial x} \frac{\partial N_j}{\partial x} + \frac{\partial N_i}{\partial y} \frac{\partial N_j}{\partial y} + \frac{\partial N_i}{\partial z} \frac{\partial N_j}{\partial z}] \, dR_e , \tag{10}$$

where R_e denotes the element region.

The vector {B} results from the surface integral in (7) and can be written for the ith surface node as

$$b_i = \int_S N_i \frac{\partial p}{\partial n} \, dS , \tag{11}$$

15

where n is a local coordinate in the direction of the outward normal. By means of this vector it is possible to apply the boundary condition on the normal pressure gradient, i.e.,

$$\frac{\partial p}{\partial n} = - \rho \frac{\partial V_n}{\partial t} = - \rho \dot{V}_n \quad , \tag{12}$$

where V_n is the fluid particle velocity normal to the boundary and ρ is the fluid density. It is noted that for a fixed boundary $V_n = 0$ and the corresponding $b_i \equiv 0$.

A 'nonreflecting' or radiation boundary condition, necessary to model numerically an infinite fluid region, was developed by Zienkiewicz and Newton [7]. They demonstrated that for a plane wave normally incident upon a plane boundary the condition to be satisfied by p on the boundary S is

$$\frac{\partial p}{\partial n} + \frac{1}{c} \dot{p} = 0 \quad . \tag{13}$$

The corresponding boundary integral (11) is

$$- \frac{1}{c} \int_S N_i \frac{\partial p}{\partial t} dS = - \frac{1}{c} \int_S N_i N_j dS \dot{p}_j \quad . \tag{14}$$

This leads to an additional "damping" term $[D]\{\dot{p}\}$ in the matrix equation (8), i.e.,

$$[Q]\{\ddot{p}\} + [D]\{\dot{p}\} + [H]\{p\} = \{B\} \quad . \tag{15}$$

16

[D] is the assembled fluid "damping" matrix defined on the element level as

$$d_{ij} = \frac{1}{c} \int_{S_e} N_i N_j \, dS_e \, ,$$ (16)

where S_e denotes the external boundary of the element.

C. THE COUPLED STRUCTURE-FLUID PROBLEM

The vectors $\{P\}$ of the force term of equation (2) and $\{B\}$ of equation (15) determine the coupling of the fluid and structure in the discretized problem. Recall from equation (3) that the nodal forces on the structure due to the pressure are

$$P_i = \int_S N_i' \, p \, dS = \int_S N_i' N_j p_j \, dS = [\int_S N_i' N_j \, dS] \, p_j$$

or

$$\{P\} = [L] \{p\} \, ,$$ (17)

where [L] is the assembled matrix of element contributions

$$\ell_{ij} = \int_{S_e} N_i' N_j \, dS_e \, .$$ (18)

From equation (12)

$$\frac{\partial p}{\partial n} = - \rho \dot{V}_n = - \rho N_j' \, \ddot{\delta}_j \, .$$ (19)

17

The forcing term {B} in equation (15) becomes

$$B_i = -\rho \int_S N_i \ N_j' \ \ddot{\delta}_j \ dS \ ,$$

or

$$\{B\} = - [S]\{\ddot{\delta}\} \ , \tag{20}$$

with [S] the assembled matrix of element contributions

$$s_{ij} = \rho \int_{S_e} N_i N_j \ dS_e \ . \tag{21}$$

Observe that

$$\rho[L]^T = [S] \ . \tag{22}$$

The complete elasto-hydrodynamic system has been
formulated and can be summarized. Rewriting equation (1)
with (2) and (17),

$$[M]\{\ddot{\delta}\} + [C]\{\dot{\delta}\} + [K]\{\delta\} = [L]\{p\} + \{F\} \tag{23}$$

describes the structure behavior. Similarly, equation (15)
with (20) and (22) can be written as

$$[Q]\{\ddot{p}\} + [D]\{\dot{p}\} + [H]\{p\} = - \rho \ [L]^T\{\ddot{\delta}\} \ . \tag{24}$$

This governs the fluid response.

The complete system of equations can be written as

$$\begin{bmatrix} M & 0 \\ \rho L^T & Q \end{bmatrix} \begin{Bmatrix} \ddot{\delta} \\ \ddot{p} \end{Bmatrix} + \begin{bmatrix} C & 0 \\ 0 & D \end{bmatrix} \begin{Bmatrix} \dot{\delta} \\ \dot{p} \end{Bmatrix} + \begin{bmatrix} K & -L \\ 0 & H \end{bmatrix} \begin{Bmatrix} \delta \\ p \end{Bmatrix} = \begin{Bmatrix} F \\ 0 \end{Bmatrix} . \quad (25)$$

Using general finite element techniques it is possible to generate and subsequently solve this unsymmetrical system of equations for the submarine-fluid problem under consideration. However, an alternative method based on this general formulation will be utilized to effect a solution using the following superposition theorem.

D. SUPERPOSITION THEOREM

It will be shown that the coupled elasto-hydrodynamic problem formulated above may be solved in two stages and that the structure response thus found is the same as in the complete unseparated problem. In the first stage the structure is constrained against responding to the loading imposed by the incident pressure pulse. In the second stage the structure and the fluid are initially at rest. External loads are applied to the structure to simulate the loading by the pressure pulse of the first stage and the structure and fluid responses are found.

1. The Complete Problem

Equations (23) and (24) govern the structure and fluid response subject to the initial conditions

19

$$\{\delta(0)\} \quad = \quad \{\dot{\delta}(0)\} \quad = \quad 0 \quad , \tag{26}$$

$$\{p(0)\} \quad = \quad \{a\} \quad , \quad \{\dot{p}(0)\} \quad = \quad \{b\} \quad , \tag{27}$$

where $\{a\}$ and $\{b\}$ are given vectors. It is assumed that

$$\{F\} \quad = \quad 0 \quad . \tag{28}$$

The solution of the complete problem requires that equations (23) and (24) with equation (28) be solved for $\{\delta(t)\}$ and $\{p(t)\}$, subject to the initial conditions, equations (26) and (27).

2. Stage One

The dependent variables will be $\{p^{(1)}(t)\}$ and $\{\delta^{(1)}(t)\}$. Recall that in the first stage the structure is constrained against motion, i.e.,

$$\{\ddot{\delta}^{(1)}(t)\} \equiv 0 \quad . \tag{29}$$

For the fluid, equation (24) becomes

$$[Q]\{\ddot{p}^{(1)}\} + [D]\{\dot{p}^{(1)}\} + [H]\{p^{(1)}\} \quad = \quad 0 \quad , \tag{30}$$

with the initial conditions

$$\{p^{(1)}(0)\} = \{a\} \quad , \quad \{\dot{p}^{(1)}(0)\} = \{b\} \quad . \tag{31}$$

20

Equation (23), governing the structure response, will be
satisfied by (29) if it is required that

$$\{F^{(1)}\} = - [L]\{p^{(1)}\} \ . \tag{32}$$

For the first stage one need only solve equation (30)
for $\{p^{(1)}(t)\}$ subject to the initial conditions of equation
(31). $\{F^{(1)}\}$ is subsequently found from equation (32).

3. Stage Two

The system is initially at rest and the structure is
externally loaded to simulate loading by the pressure pulse.
The dependent variables for this stage are $\{p^{(2)}(t)\}$ and
$\{\delta^{(2)}(t)\}$. For the fluid

$$[Q]\{\ddot{p}^{(2)}\} + [D]\{\dot{p}^{(2)}\} + [H]\{p^{(2)}\} = - \rho [L]^T\{\ddot{\delta}^{(2)}\} \ , \tag{33}$$

with the initial conditions

$$\{p^{(2)}(0)\} = \{\dot{p}^{(2)}(0)\} = 0 \ . \tag{34}$$

For the structure

$$[M]\{\ddot{\delta}^{(2)}\} + [C]\{\dot{\delta}^{(2)}\} + [K]\{\delta^{(2)}\} = [L]\{p^{(2)}\} + \{F^{(2)}\}, \tag{35}$$

with the initial conditions

$$\{\delta^{(2)}(0)\} = \{\dot{\delta}^{(2)}(0)\} = 0 \ . \tag{36}$$

21

Specify further that

$$\{F^{(2)}\} = - \{F^{(1)}\} \ . \tag{37}$$

For the second stage of the solution it is necessary to solve equations (33) and (35) for $\{p^{(2)}(t)\}$ and $\{\delta^{(2)}(t)\}$ with equation (37) subject to the initial conditions of equations (34) and (36).

4. Superposition

It is now asserted that

$$\{p(t)\} = \{p^{(1)}(t)\} + \{p^{(2)}(t)\} \ , \tag{38}$$

and

$$\{\delta(t)\} = \{\delta^{(1)}(t)\} + \{\delta^{(2)}(t)\} \ . \tag{39}$$

In virtue of the conditions imposed on the first stage pressures $\{p^{(1)}(t)\}$ and displacements $\{\delta^{(1)}(t)\}$, equations (29) - (32), and on the second stage pressures $\{p^{(2)}(t)\}$ and displacements $\{\delta^{(2)}(t)\}$, equations (33) - (37), it follows that $\{p(t)\}$ and $\{\delta(t)\}$ as given by equations (38) and (39) satisfy the governing equations for the complete problem, equations (25) - (28). This establishes the superposition theorem for the coupled elasto-hydrodynamic problem.

Implementation of the superposition theorem does not require that the rigid body pressure distribution or the structure response be obtained by the finite element method.

It is noted that for the submarine structural model under consideration a three-dimensional analysis is necessary. However, the superposition theorem permits the rigid body pressure distribution to be obtained from a two-dimensional analysis.

III. WAVE PROPAGATION BY THE FINITE ELEMENT METHOD

To evaluate numerically the interaction of a wave with
a structure it is necessary to propagate the blast wave
through the contiguous fluid region. Before proceeding with
the complicated two-dimensional interaction of a blast wave
with a rigid cylindrical structure, the characteristics of
the one-dimensional wave propagation are studied. The
techniques developed and utilized for the one-dimensional
case are subsequently employed in the two-dimensional study.

A. ONE-DIMENSIONAL WAVE PROPAGATION

The numerical results obtained by the finite element
method for the one-dimensional wave propagation problem are
easily compared to well known theoretical values and thus
provide insight into the behavioral characteristics of the
techniques employed.

The physical situation to be considered is a semi-infinite
fluid strip of unit cross-sectional area. Through this region
a pressure wave of known shape is propagating with acoustic
velocity c. A rigid structure is located at $x = 0$ and the
radiation boundary condition is applied at $x = L$. Equation
(24), with $\{\delta(t)\} = 0$,

$$[Q]\{\ddot{p}\} + [D]\{\dot{p}\} + [H]\{p\} = 0 \quad , \tag{40}$$

governs the fluid response for the case. The initial

conditions $\{p(0)\}$ and $\{\dot{p}(0)\}$ are determined by the wave form under consideration.

1.   Blast Wave Model

A blast wave, which is generated by an underwater explosion, is characterized by an extremely rapid rise in pressure to a maximum value p*, followed by decreasing pressure. For the purpose of investigating blast wave propagation it would appear that a step pulse of finite duration would be a satisfactory wave model. However, it is evident that to model a moving discontinuous function by a finite fixed spatial discretization is not possible. Consequently, for the purpose of this investigation the blast wave is modeled as a ramp rise to a constant value, i.e., a ramp-step wave. Although the ramp-step wave is of primary interest, this investigation is not limited exclusively to that wave form and illustrative results of tests made using different wave forms are also given later.

2.   Element Selection

To study a significant portion of a blast wave, which is propagating at the acoustic velocity, requires a spatial domain of considerable extent. This is necessary to avoid spurious effects caused by reflections from the (artificial) boundaries. Accordingly, the required linear dimensions of the region are approximately proportional to the time interval during which the structure-fluid response is sought. It is evident that, if a fine subdivision of the one-dimensional fluid strip is required to represent the wave form under

25

consideration, the number of degrees of freedom in equation
(40) may become prohibitively large when the same subdivision
is applied to the two-dimensional region.

Two types of finite elements, linear and cubic, are
considered for the spatial discretization of equation (40).
As their names imply they respectively provide for a linear
and cubic variation of the pressure within an element. When
propagating smooth wave forms represented by a significant
number of elements, e.g., $p(x) = p^* \sin^2(\pi x/L)$ or
$p(x) = p^* \cos(\pi x/L)$, both the linear and cubic elements
produce excellent numerical results. However, in choosing
the type of finite element best suited to represent spatially
a propagating blast wave it is necessary to consider: a) the
general shape of the wave; and b) two instantaneous finite
element representations of the wave front as it propagates
across a region.

As established above, the general shape of the wave
of primary interest is the ramp-step wave. For the second
consideration, assume that the node spacing s_n is equal for
both element types. Due to the character of the linear and
cubic elements note that three linear elements are required
for each cubic element in the spatial representation of the
wave front. Now consider a ramp wave front that at one
instant in time is represented spatially by four nodal values,
i.e., the ramp rise spans one cubic element. At this
particular instant both element types are capable of an exact
representation of the ramp wave front. For the second instant

in time, let the wave advance a distance equal to one node
space. At this instant of time the linear elements continue
to provide an exact representation of the wave front.
However, when the wave is in this spatial position relative
to the cubic elements, they are required to fit a cubic
polynomial through a function which has a discontinuous first
derivative. This results in a distortion of the wave front.

The above qualitative discussion explains the
observed superior performance of the linear element when
used in the spatial discretization of equation (40). It also
serves as a reminder that higher order finite elements per
se do not guarantee superior results and may indeed lead to
poorer results.

3. Time Integration

The time integration of the governing equation (40)
is computed using two finite differencing techniques, the
Newmark-β method as adapted by Chan, Cox and Benfield [10]
and the Houbolt method [11]. Both provide a numerical method
of determining the time dependent response of a differential
equation of the form

$$m\ddot{w} + d\dot{w} + kw = f(t) \quad , \tag{41}$$

where m, d and k are constants. The difference equation
proposed by Chan, et al. [10] is

$$(m + \frac{h}{2} d + \beta h^2 k)w_n = (2m - (1-2\beta)h^2 k)w_{n-1}$$

$$- (m - \frac{h}{2} d + \beta h^2 k)w_{n-2} + \beta h^2 (f_n + (\frac{1}{\beta} - 2)f_{n-1} + f_{n-2}) , \tag{42}$$

27

where h is the time step and β is a parameter which may have
any value from 0 to 1/4. The value β = 1/12 is chosen for
calculations using the stability requirements established by
Newmark [12].

The starting equation is

$$(m + \frac{h}{2} d + \beta h^2 k)w_1 = (m + \frac{h}{2} d - (\frac{1}{2} - \beta)h^2 k - (\frac{1}{4} - \beta) \frac{h^3 dk}{m}) w_0$$

$$+ (m - (\frac{1}{4} - \beta)\frac{h^2 d^2}{m}) h\dot{w}_0 + \beta h^2 f_1$$

$$+ ((\frac{1}{12} - \beta) + (\frac{1}{4} - \beta) \frac{hd}{m}) h^2 f_0 , \qquad (43)$$

where w_0 and $\dot{w}_0$ are initial values.

The Houbolt method [11] is developed from a consider-
ation of a cubic curve that passes through four successive
ordinates to obtain the difference equation

$$(2m + \frac{11}{6} dh + kh^2)w_n = (5m + 3dh)w_{n-1} - (4m + \frac{3}{2} dh)w_{n-2}$$

$$+ (m + \frac{1}{3} dh)w_{n-3} + h^2 f_n . \qquad (44)$$

The starting procedure for the Houbolt method employed
in the one-dimensional propagation problem is as follows:
assume that the wave form is known at t = 0 and that the wave
is propagating undeformed through the fluid region with the

acoustic velocity c. The pressure distribution p can be
described as

$$p(x,t) = f(x + ct) \qquad\qquad (45)$$

for a wave moving in the negative x-direction. It is apparent
that once the wave form is specified at t = 0 as a function
of x the required preceding values of pressure may be calcu-
lated directly from equation (45) and thus provide exact
starting values for equation (44).

It is noted that the Houbolt method is theoretically
stable for all step sizes, while the Newmark-β method becomes
unstable if the limiting step size established by Newmark [12]
is exceeded.

As an example of the results obtained by the methods
outlined above consider a fluid strip in which the acoustic
velocity c = 5000 ft/sec. The region of interest extends
5000 ft. from a rigid structure located at x = 0 and is
divided by 31 equally spaced nodes. The integration time
step h = 0.01 sec. At time t = 0 the wave form has the shape
and position in the region shown in Fig. 1. As the wave
strikes the rigid structure at x = 0 it is reflected and
propagates to the right where the radiation boundary condition
is applied.

After 100 time steps (t = 1.0 sec.) the wave will be
positioned as shown in Fig. 2. The corresponding numerical
results are shown for the Newmark-β integration with cubic
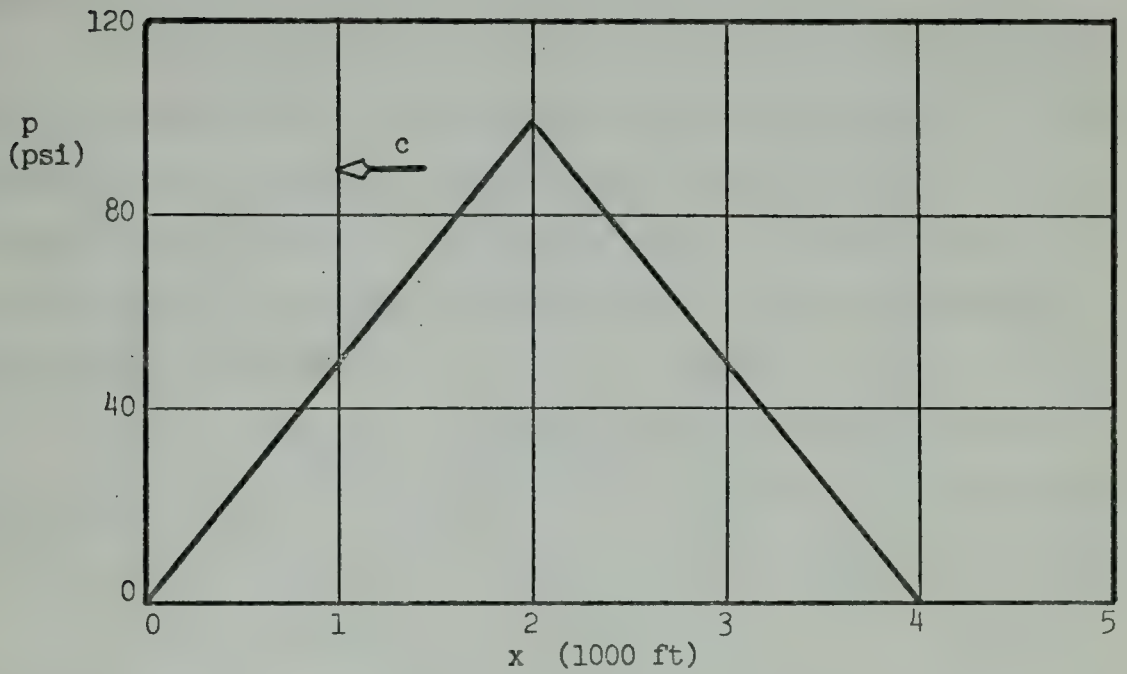elements and the Houbolt integration - linear element

29
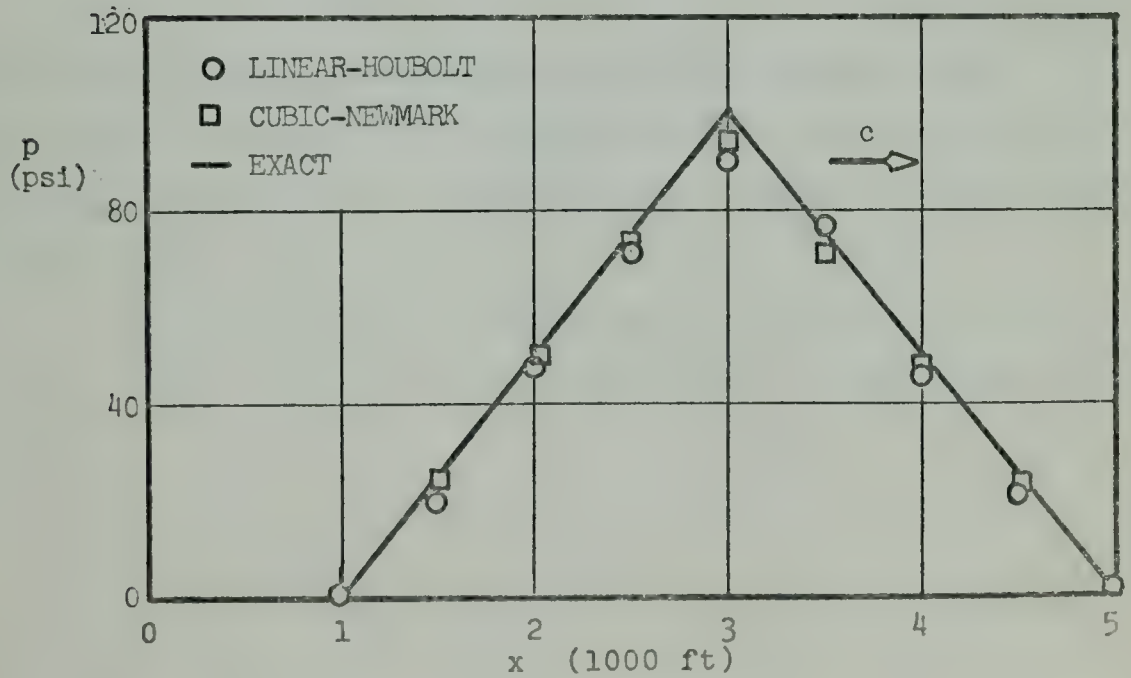
Fig. 1. Pressure-vs.-distance at t = 0

Fig. 2. Pressure-vs.-distance after 100 time steps

30

combination. The other combinations of integration techniques
and elements give essentially identical results.

It is evident that to determine the optimum integra-
tion technique it is necessary to establish criteria to judge
the results of tests. The criteria chosen are: a) the
pressure-time history at the structure-fluid interface
(impulse) and b) retention of wave shape after propagation
through the fluid.

If the rise time τ_r of the ramp is chosen as the
parameter necessary to describe the wave front, criteria for
selecting the time h and the node spacing s_n can be developed.

Assume that to describe the slope of the ramp rise
at least two linear elements are required, i.e.,

$$\tau_r \geq \frac{2s_n}{c} \ . \tag{46}$$

Intuitively this restriction on the node spacing seems
reasonable because it will provide that at least two spatial
locations in the fluid strip are used to describe the slope
of the ramp.

It also seems reasonable to restrict the time step
in such a way that the wave front cannot cross an element in
one step, i.e.,

$$h < \frac{s_n}{c} \ . \tag{47}$$

31

The above restrictions are proposed as a general guide in the initial selection of the nodal spacing and the integration time step. They are not intended to establish restrictions which cannot be violated. As shown below, satisfactory results may be obtained when the restriction on τ_r (46) is violated.

Using the criteria established above to judge the effectiveness of the integration technique, numerous tests were made to determine which time integration technique is better suited for the purpose of propagating a ramp-step wave.

Consider, for example, a triangular shape wave that has the following characteristics:

$$h = \frac{1}{2} \frac{s_n}{c} \quad ,$$

$$\tau_r = \frac{s_n}{c} \quad ,$$

$$\tau_d = 19 \frac{s_n}{c} \quad ,$$

where τ_d is the time required for the wave to decay from the maximum value $\dot{p}^*$ to zero. The pressure-time histories at the rigid structure-fluid interface obtained by both integration methods are shown in Fig. 3. The result shown in Fig. 4 is obtained by employing a cubic finite element discretization with the Houbolt integration technique for the same wave form.

Consider a ramp-step wave with the characteristics:

$$h = \frac{1}{2} \frac{s_n}{c} \quad , \quad \tau_r = 2 \frac{s_n}{c} \quad .$$

32
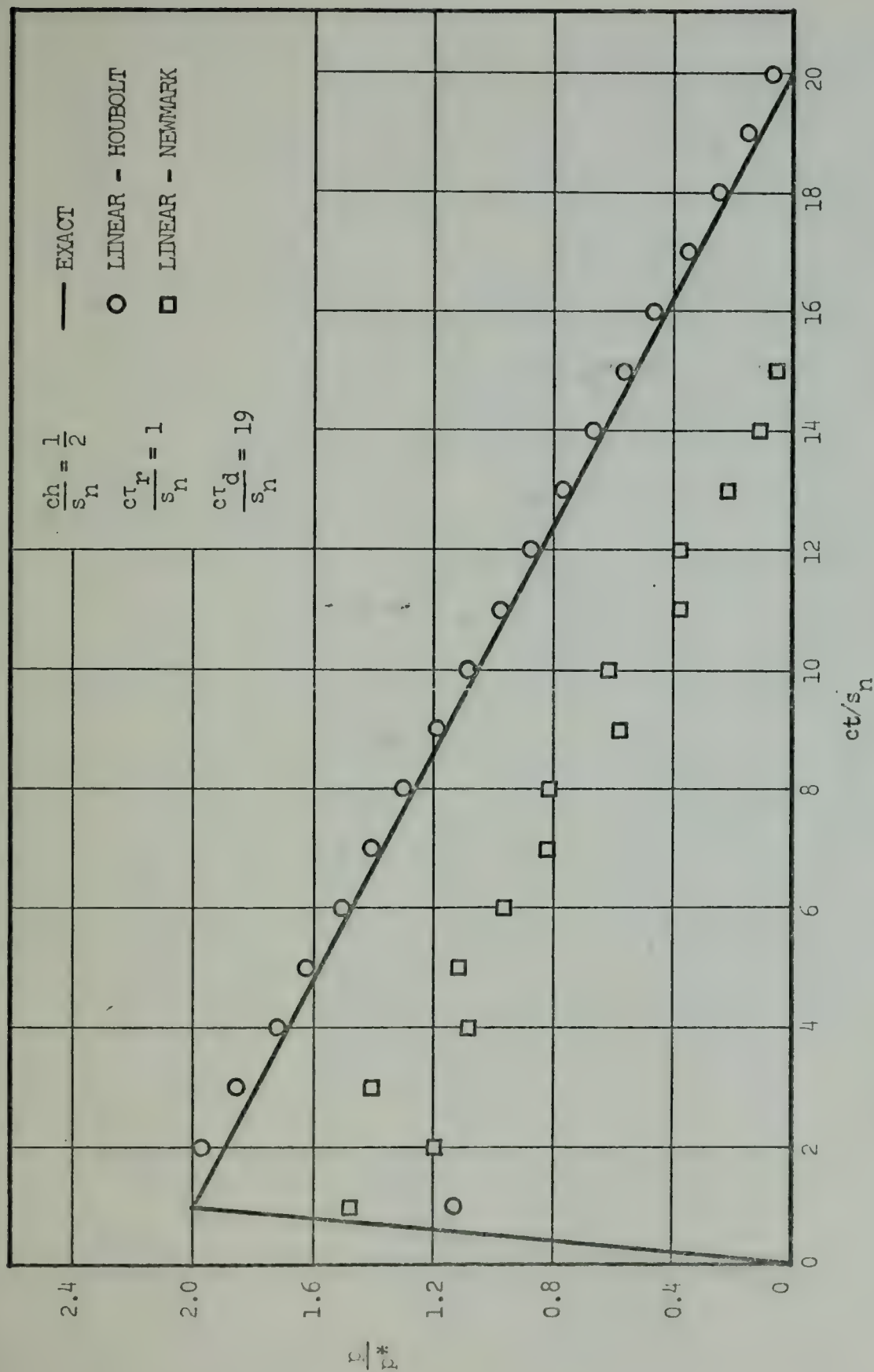
Fig. 3. Pressure-vs.-Time at the Rigid Structure-Fluid Interface
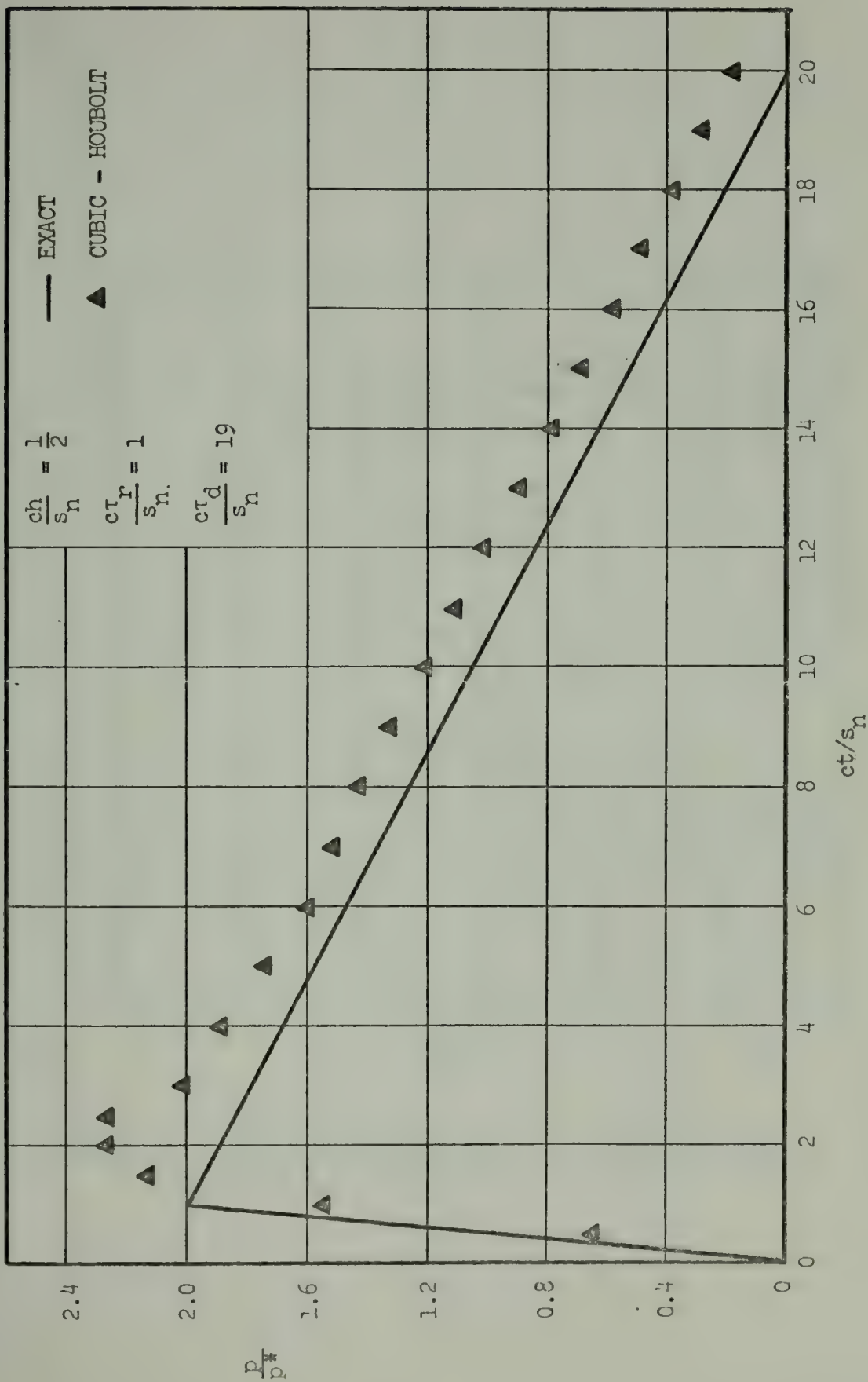
Fig. 4. Pressure-vs.-Time at the Rigid Structure-Fluid Interface

34
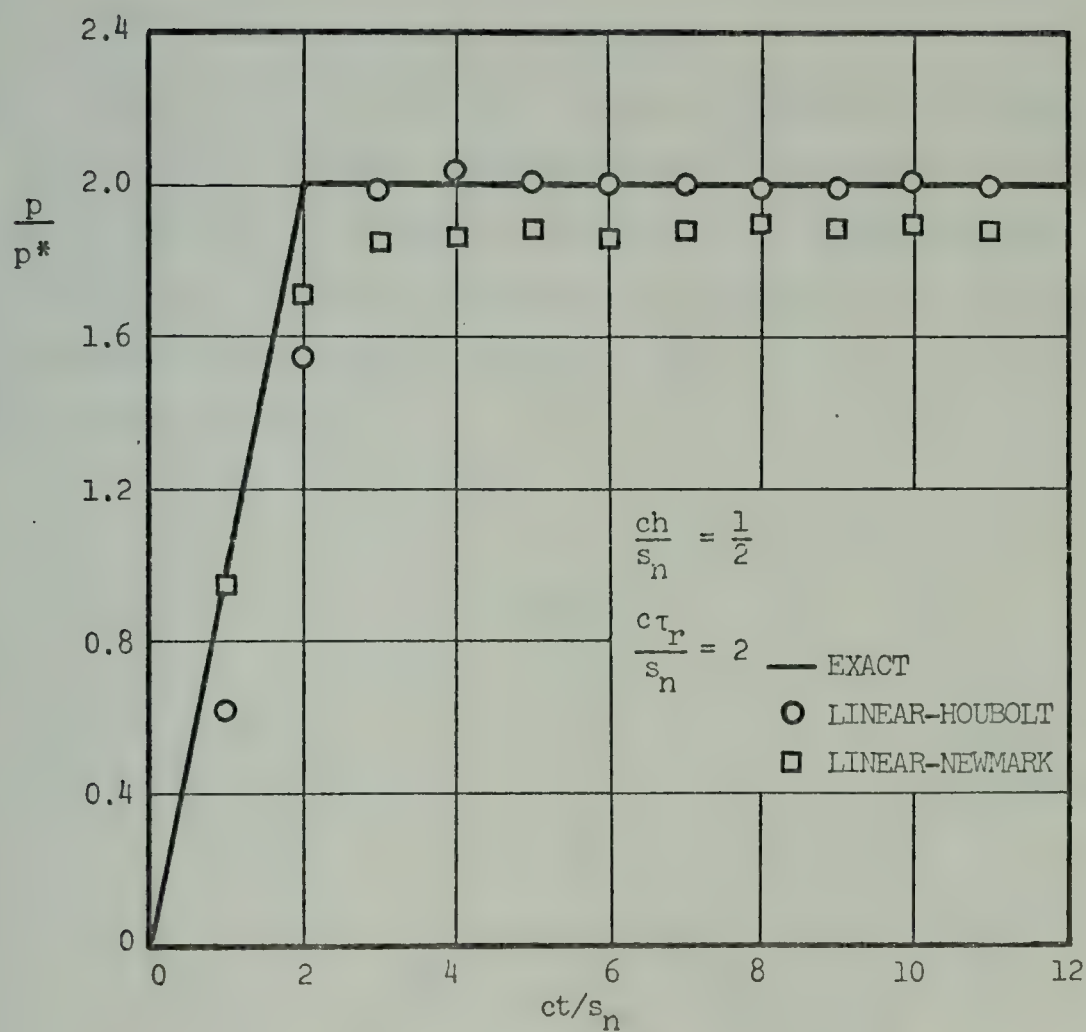
Fig. 5. Pressure-vs.-Time at the Rigid Structure-
Fluid Interface (ramp-step wave).

The resulting pressure-time histories at the fluid-structure interface are shown in Fig. 5. From this and other results it is concluded that the Houbolt integration technique is better suited for the propagation of the blast wave through a fluid region.

B.   TWO-DIMENSIONAL WAVE PROPAGATION

Based upon the results of the one-dimensional study, the linear finite element and the Houbolt integration technique are selected to evaluate numerically the pressure-time history at the rigid cylindrical structure-fluid interface resulting from a ramp-step wave. The geometry of the problem is shown in Fig. 6.
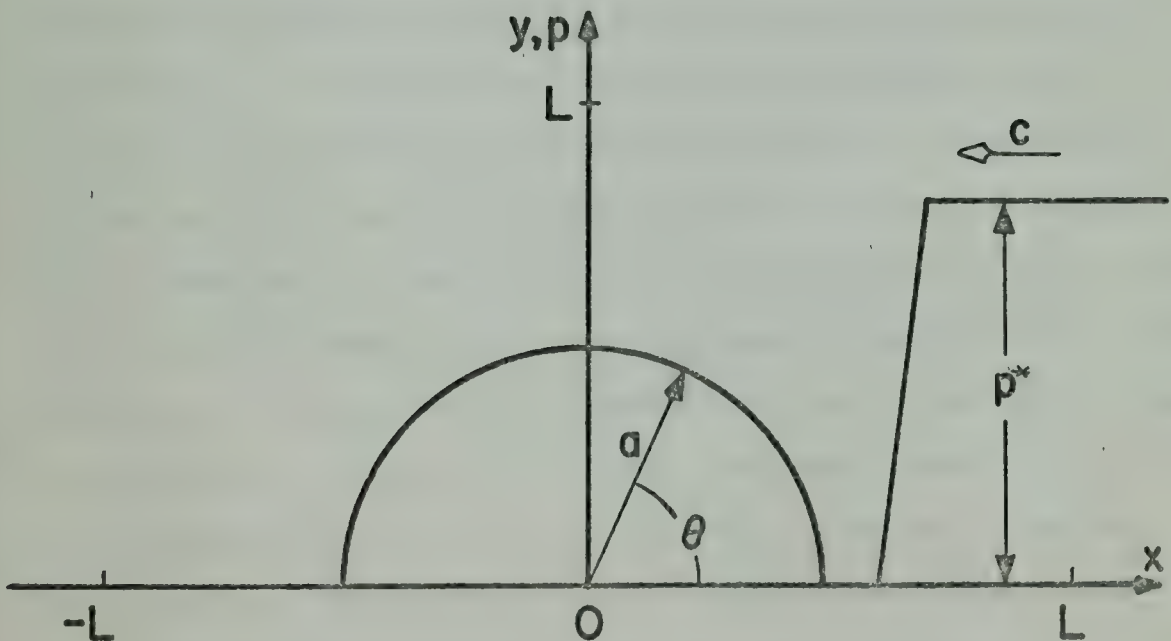
Fig. 6.   Two-dimensional geometry

The rigid cylindrical structure, of radius a, is centered at the origin of the x,y coordinate system. The diagrammatically shown ramp-step wave is propagating through the fluid in the negative x-direction with the acoustic velocity c. Due to symmetry only the upper half plane is shown and the rigid body boundary condition is applied along the x-axis. The additional necessary boundary and initial conditions are specified below. It is convenient to define a nondimensional time parameter $\tau = ct/a$, where $\tau = 0$ is the time of incidence of the wave at $r = a$, $\theta = 0°$.

1. Boundary Conditions

The radiation boundary condition as developed earlier is valid only for a plane wave normally incident upon a plane boundary. Clearly the wave reflected from the rigid cylinder will not be normally incident upon the far fluid boundaries. It is necessary that these boundaries be located a sufficiently large distance from the structure to insure that the results at the interface are not affected. This investigation and Sette's [1] results both indicate that the transient response of the blast wave-cylindric structure interaction is essentially completed in 8a/c time units after incidences at $r = a$, $\theta = 0°$. As a consequence the far fluid boundaries are located sufficiently far from the structure to prevent any boundary reflected waves from reaching the structure in the time specified. For programming convenience the rigid body boundary condition is applied to the boundary at $y = L$ and the radiation boundary condition is applied at $x = \pm L$.

A significant characteristic of the radiation boundary condition was observed during the two-dimensional study. It was observed that if the constant value portion of the ramp-step wave is applied to the boundary nodes at x = L for three successive time increments, then the radiation boundary condition continued to let the wave enter the fluid region of interest. In addition the interaction of the wave reflected from the structure with the boundary does not affect the incoming wave. This observation permitted a significant reduction of the fluid region under consideration, resulting in a proportionate reduction in the number of degrees-of-freedom required for the spatial discretization of equation (40).

2. Two-Dimensional Mesh Consideration

In considering the two-dimensional spatial representation (mesh) of the fluid field by the finite element method, it is necessary to incorporate both the physical geometry and the wave propagation aspects of the problem. As described in the one-dimensional study the integration time step is logically limited by the node spacing. Equation (47) governs this dependence. The physical dimension of the cylindric structure, when considered in the context of the advancing wave front, also restricts the nodal spacing. Clearly, if the node spacing s_n and structure radius "a" are chosen to be of the same order of magnitude and the upper limit on the time step is utilized, the wave front could advance across the structure in a few time steps and the pressure-time history at the interface would be of suspect value. It is

38

therefore necessary to produce a mesh which affords a degree
of fineness near the structure compatible with the integration
time step and wave characteristics. Additionally, computer
storage and processing time restrictions must be considered.

After extensive experimentation the mesh shown in
Fig. 7 was developed. Due to geometric symmetry about the
y-axis only the region of the first quadrant is shown. This
mesh has the following notable characteristics:

a) Elements which form the cylindrical structure boundary
   are 'special' 5 noded, linear-parabolic elements. At
   the interface the 'special' elements represent the
   rigid boundary by a parabolic arc and provide for a
   transition to the linear elements in the fluid field.
   The interface nodes are equally spaced at angular
   intervals of 7.5°.

b) The 'near fluid' region is characterized by a radial
   node spacing equal to the 'far fluid' node spacing and
   an angular node spacing of 15°.

c) The transition from the cylindrical 'near fluid' region
   to the rectangular 'far fluid' region is accomplished
   with a minimum number of distorted and degenerate
   elements.

d) The uniform rectangular 'far fluid' region is charac-
   terized by node spacing $s_n = \frac{1}{2} a$. The appropriate
   boundary conditions as discussed above are applied at
   $x = \pm 6a$ and at $y = 6a$.
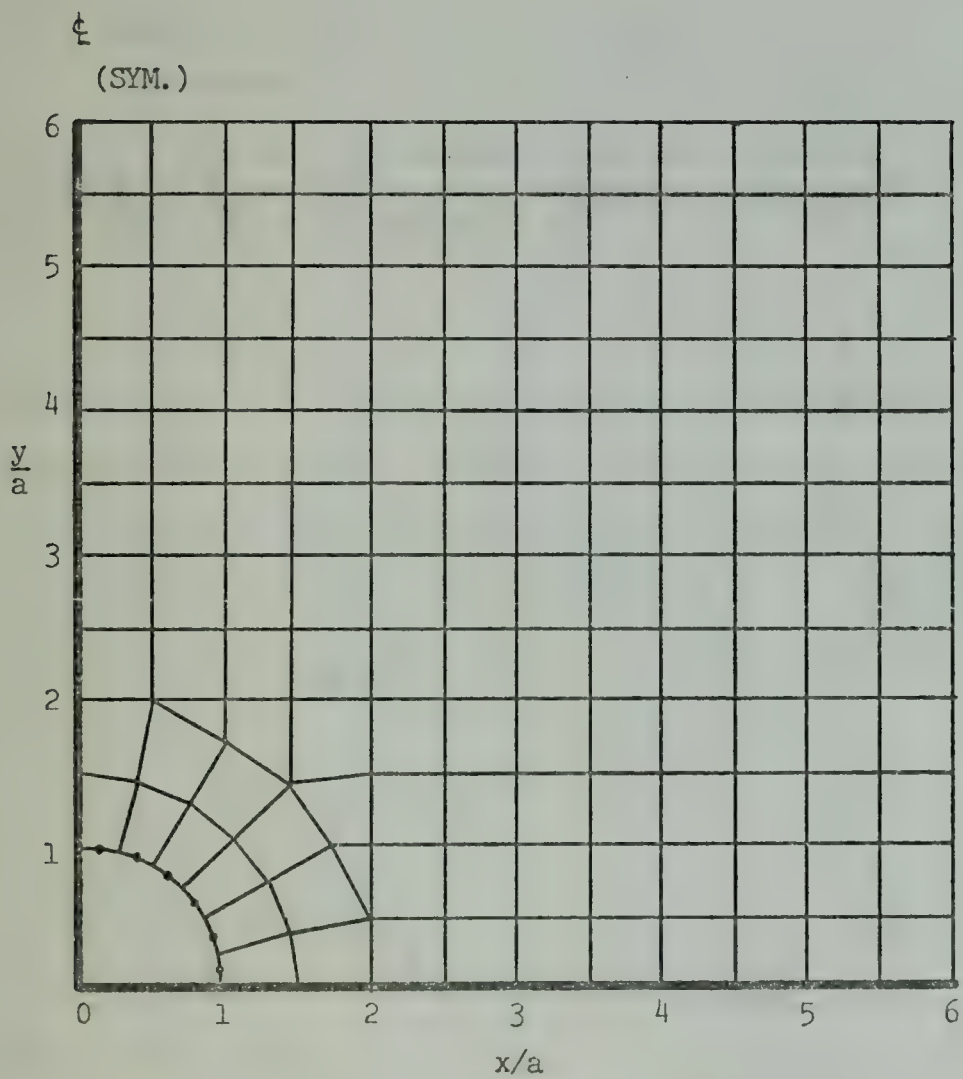
Fig. 7.   Two-Dimensional Finite Element Mesh

The overall characteristic of the mesh is element size uniformity. Results indicate that such uniformity in both spatial directions is desirable for satisfactory two-dimensional wave propagation.

3. Integration Starting Procedure

The Houbolt integration starting procedure, equation (45), used for the one-dimensional case assumed a general solution of the wave equation (4) of the form

$$p(x,t) = f(x + ct) + g(x - ct) \tag{48}$$

with $g(x - ct) = 0$. This solution is valid assuming that $f'(x)$ and $f''(x)$ exist. However, the ramp-step wave has a discontinuous first derivative and singular higher derivatives. To avoid this inconsistency assume that the ramp wave front takes the form of a cubic curve at $t = 0$.

$$p = \frac{p^*}{2} + \alpha x' + \beta (x')^3 \ , \tag{49}$$

with $\frac{\partial p}{\partial x} = \alpha + 3\beta (x')^2 \ , \tag{50}$

where $x' = x - x_0$.

If $p = p^*$ and $\frac{\partial p}{\partial x} = 0$ at $x' = \xi$ as shown in Fig. 8 it is then possible to solve equations (49) and (50) for the unknown coefficients
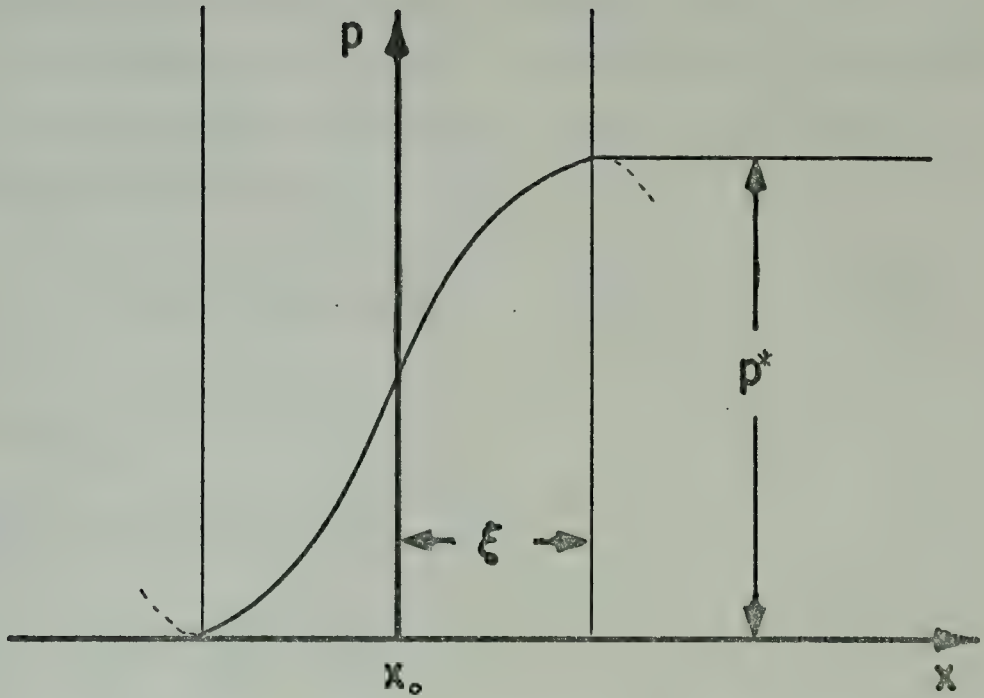
Fig. 8. Cubic Wave Front

$$\alpha = \frac{3p^*}{4\xi} , \qquad \text{and} \qquad \beta = - \frac{p^*}{4\xi^3} ,$$

or

$$p = \frac{1}{2} p^* \left(1 + \frac{3}{2} \frac{x'}{\xi} - \frac{1}{2} \left(\frac{x'}{\xi}\right)^3 \right) . \qquad (52)$$

By substituting into (48) and differentiating with respect to time

$$\dot{p}\Big|_{t=0} = \frac{3}{4} \frac{p^*}{\xi} c \left(1 - \left(\frac{x'}{\xi}\right)^2 \right) . \qquad (53)$$

Equations (52) and (53) determine the initial conditions
necessary for a proper formulation of the boundary value
problem in the region of the cubic ramp wave front.

To incorporate the initial conditions into a starting
procedure for the Houbolt integration technique consider a
Taylor series expansion about $t = 0$

$$p = p_0 + \dot{p}_0 t + \frac{1}{2}\ddot{p}_0 t^2 \quad , \tag{54}$$

where p_0 is $p\big|_{t=0}$.

If h is the time step

$$p_{-1} = p_0 - h\dot{p}_0 + \frac{h^2}{2}\ddot{p}_0 \quad ,$$

$$\tag{55}$$

$$p_{+1} = p_0 + h\dot{p}_0 + \frac{h^2}{2}\ddot{p}_0 \quad .$$

The vector $\{\ddot{p}_0\}$ is deduced from equation (40), i.e.,

$$\{\ddot{p}_0\} = [Q]^{-1} (-[C]\{\dot{p}_0\} - [H]\{p_0\}) \quad . \tag{56}$$

Thus, equations (55) with equations (56), (52) and (53)
provide a consistent starting procedure for the two-
dimensional propagation problem employing the Houbolt
integration technique.

To minimize errors in the numerical solution of the
pressure-time history, the wave front is positioned in the
fluid so that at $t = 0$ the cubic-ramp has its initial (leftmost)
point at $r = a$, $\theta = 0°$.

4. Results

Consider the following integration, wave and mesh characteristics:

$$h = \frac{a}{6c} \, ,$$

$$\tau_r = \frac{0.97a}{c} \, ,$$

$$s_n = \frac{1}{2} a \; .$$

Implementation of boundary conditions, mesh and starting procedures described above results in the pressure-time histories at $\theta = 0°$ and $\theta = 180°$, shown in Figs. 9 and 10. The solid line represents Sette's [1] results displaced along the time axis to coincide with the incidence of the constant portion of the cubic ramp-step wave. Additional curves are given for $\theta = 30°, 60°, 90°, 120°, 150°$ in Appendix A. No comparison is available for the curves given for 120° and 150°. Tabulated values of pressure vs. time at each structural node are given in Appendix B. Figures 11 and 12 provide a comparison of results when the time step is increased to $h = \frac{a}{3c}$ and the rise time decreased to $\tau_r = \frac{0.80 \, a}{c}$.

The results shown in Figs. 9 and 10 and Appendix A are in good agreement with those calculated by Sette [1]. This agreement establishes that the Houbolt [11] integration technique and the linear finite element are a suitable combination for evaluating numerically the interaction of a blast wave with a rigid cylinder.

Fig. 9. Pressure-vs.-Time at the Rigid Cylinder-
Fluid Interface ($\theta = 0°$)

Fig. 10. Pressure-vs.-Time at the Rigid Cylinder-Fluid Interface ($\theta = 180°$)
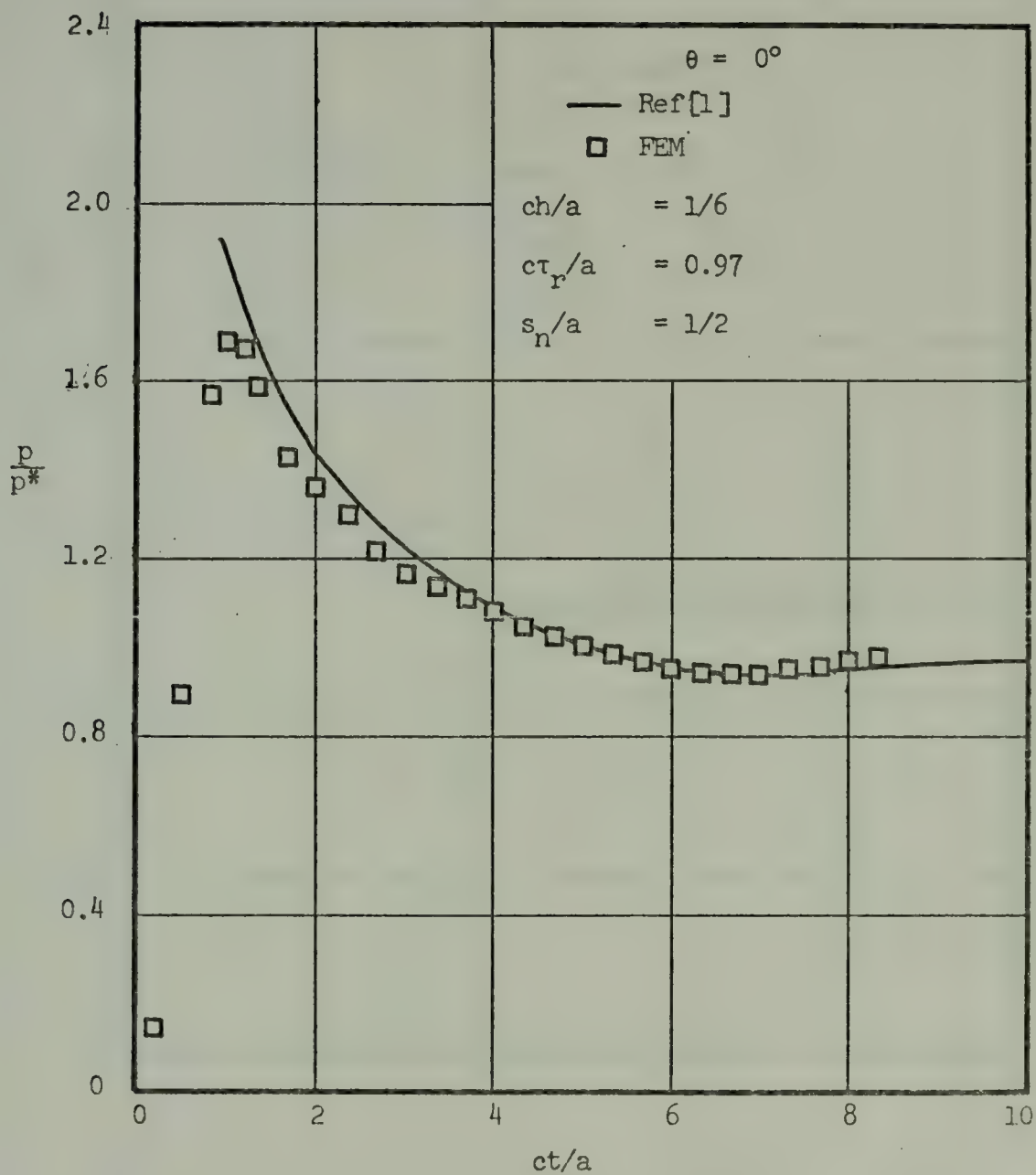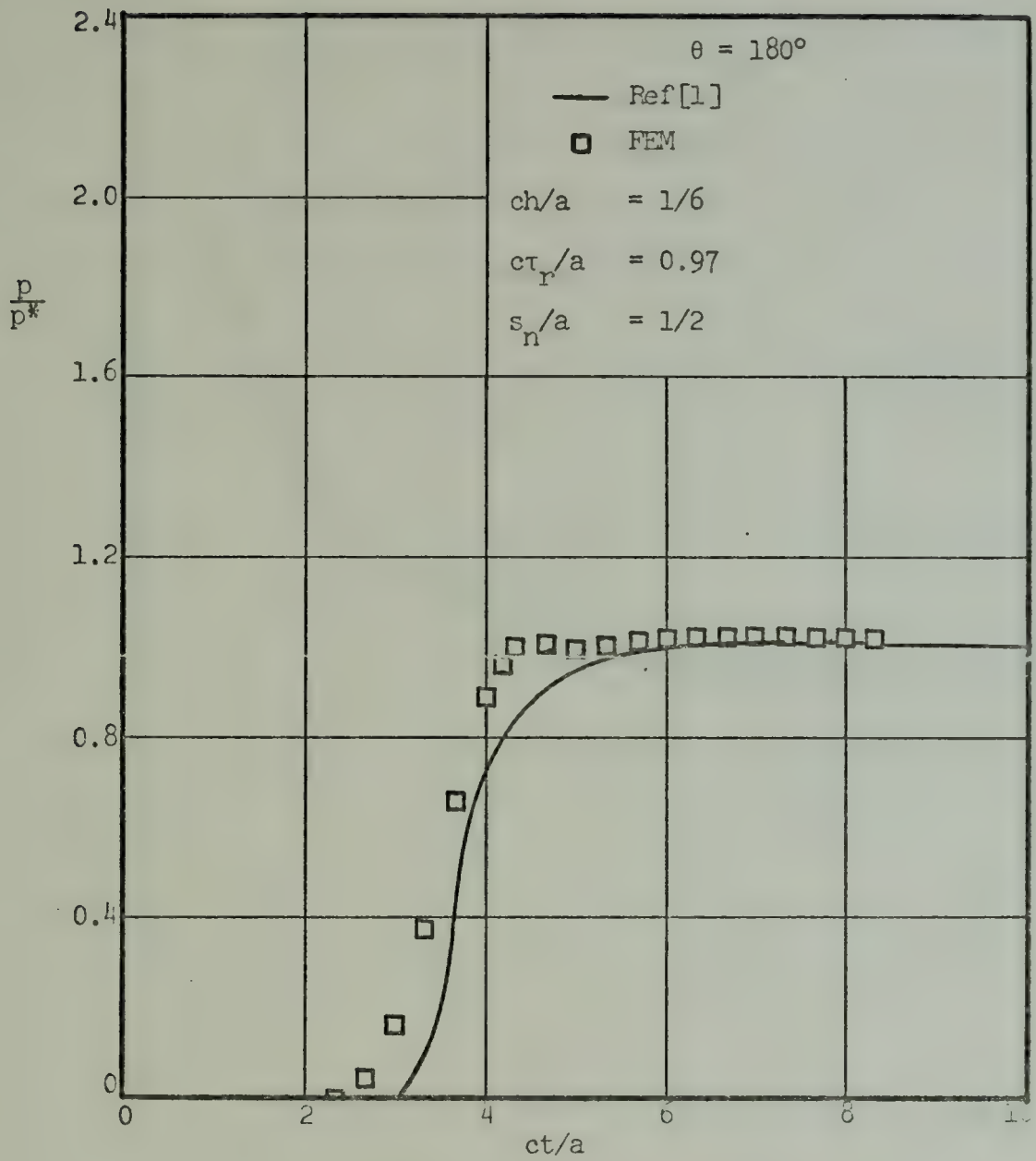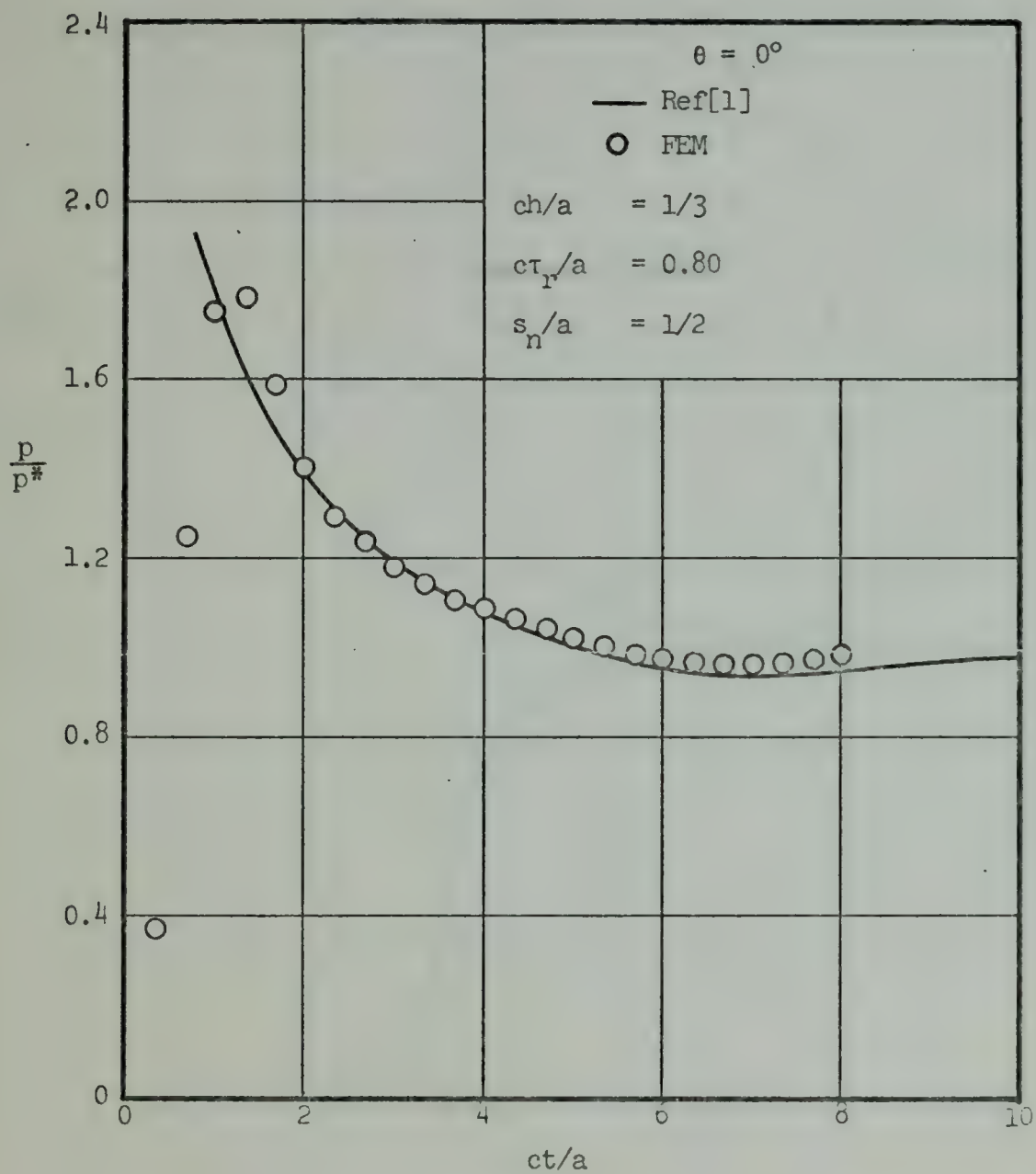
Fig. 11. Pressure-vs.-Time at the Rigid Cylinder-
Fluid Interface ($\theta = 0°$)
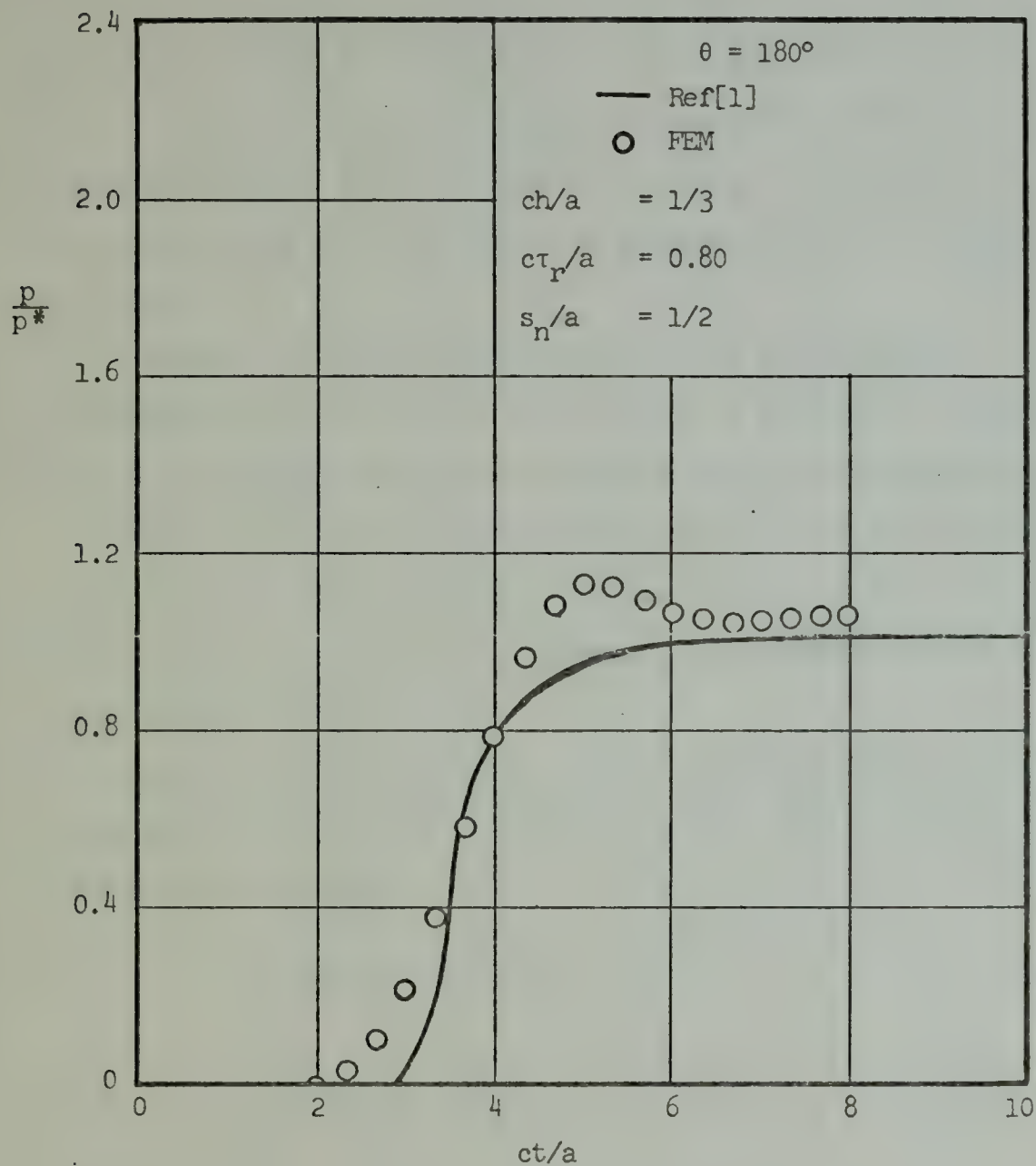
Fig. 12.   Pressure-vs.-Time at the Rigid Cylinder-
Fluid Interface (θ = 180°)

IV. THE SUBMARINE STRUCTURAL MODEL

A simple three degree-of-freedom submarine structural model is developed. This model demonstrates the implementation of the superposition theorem using the pressure-time history obtained from the two-dimensional finite element solution of the interaction of a blast wave with a rigid cylinder.

A single, ring reinforced section of a submarine, terminated at both ends by bulkheads, is modeled. The effects of the stiffening rings are included by treating the shell as orthotropic. Each bulkhead is rigid in its own plane. The added mass effect due to the surrounding water is included by considering the water to be incompressible and using strip theory.

The three modes considered are: 1) rigid body mode, 2) shear beam mode and 3) buckling mode. The equations of motion take the form

$$[M]\{\ddot{q}\} + [K]\{q\} = \{f\} \quad , \tag{57}$$

where $[M]$ and $[K]$ are the structural mass and stiffness matrices respectively, $\{q\}$ the vector of generalized displacements and $\{f\}$ the vector of generalized forces.

A point on the shell, Fig. 13, is located by specifying z and θ.
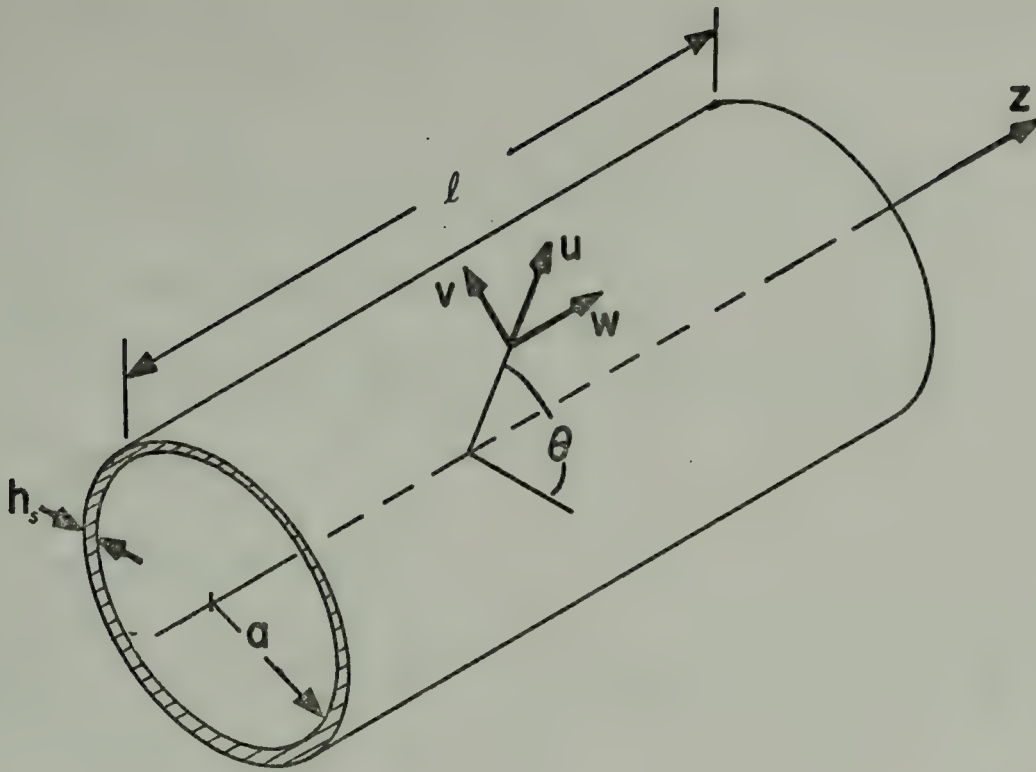
Fig. 13.   Submarine Structure Geometry

The following symbols are used to describe the structure model:

a   =   shell radius,
h_s =   shell thickness
ℓ =   bulkhead spacing,
u   =   radial displacement
v   =   tangential displacement
w   =   axial displacement
E   =   Young's modulus of elasticity,
G   =   shear modulus of elasticity
ν =   Poisson's ratio.

Values of the structural parameters used in calculations are specified in Appendix C.

The generalized modal displacements are defined as:

1) Rigid body mode,

$$u = -q_1 \cos \theta \; , \quad v = q_1 \sin \theta \; , \quad w = 0 \; . \tag{58}$$

2) Shear beam mode,

$$u = -q_2 \sin \frac{\pi z}{\ell} \cos \theta \; , \quad v = q_2 \sin \frac{\pi z}{\ell} \sin \theta \; ,$$

$$w = 0 \; . \tag{59}$$

3) Buckling mode,

$$u = -q_3 \sin^2 \frac{\pi z}{\ell} \cos 2\theta \quad , \quad v = \frac{1}{2} q_3 \sin^2 \frac{\pi z}{\ell} \sin 2\theta \; ,$$

$$w = \lambda q_3 \sin \frac{2\pi z}{\ell} \cos 2\theta \quad . \tag{60}$$

The parameter λ is evaluated by minimizing the modal strain energy.

In the rigid body mode and the shear beam mode, each cross-section (z = constant) moves as a rigid body in the athwartship direction. In the buckling mode a cross-section is deformed, but the tangential strain $\varepsilon_\theta = 0$.

A.   ADDED MASS EFFECTS

Conceptually the effects of fluid pressure p_m resulting from the radial motion of the structure should be assigned to the generalized force vector. It will be shown that the corresponding components are linear functions of $\ddot{q}_1$, $\ddot{q}_2$ and $\ddot{q}_3$ so that it is appropriate to include these effects by augmentation of the mass matrix.

51

Consider first a shell segment of infinitesmal length (dz) for which the radial displacement is

$$u = u_1 \cos \theta + u_2 \cos 2\theta \quad , \tag{61}$$

where

$$u_1 = -q_1 - q_2 \sin \frac{\pi z}{\ell} \quad , \tag{62}$$

and

$$u_2 = -q_3 \sin^2 \frac{\pi z}{\ell} \quad . \tag{63}$$

The pressure p_m exerted on the hull as a result of radial motion is determined using potential theory. For an incompressible fluid

$$\nabla^2 p_m = 0 \quad . \tag{64}$$

Let

$$p_m = p_1 + p_2 \quad . \tag{65}$$

If

$$p_1 = p_0 \frac{a}{r} \cos \theta \; f(t) \quad , \tag{66}$$

and

$$p_2 = p_0 \frac{a^2}{r^2} \cos 2\theta \; g(t) \quad , \tag{67}$$

then p_m satisfies equation (64).

From Euler's equation of motion for an inviscid fluid,

$$\left. \frac{\partial p_1}{\partial r} \right|_{r=a} = - \rho \, \ddot{u}_1 \cos \theta \; , \tag{68}$$

$$\left. p_1 \right|_{r=a} = \rho \, a \, \ddot{u}_1 \cos \theta \; , \tag{69}$$

where ρ is the fluid density. Similarly,

$$p_2\Big|_{r=a} = \frac{\rho a}{2} \ddot{u}_2 \cos 2\theta \quad . \tag{70}$$

Therefore, the pressure is given by

$$p_m\Big|_{r=a} = [p_1 + p_2]_{r=a} = \rho a(\ddot{u}_1 \cos \theta + \frac{1}{2} \ddot{u}_2 \cos 2\theta) \quad . \tag{71}$$

Let $\delta W_p{}'$ be the work done by the pressure p_m during a virtual displacement δu.

Then

$$\delta W_p{}' = -dz \int_0^{2\pi} p_m \delta u \, a \, d\theta \quad . \tag{72}$$

Substituting

$$\delta u = \delta u_1 \cos \theta + \delta u_2 \cos 2\theta \quad ,$$

and performing the indicated integration gives

$$\delta W_p{}' = -\pi \rho a^2 (\ddot{u}_1 \delta u_1 + \frac{1}{2} \ddot{u}_2 \delta u_2) \, dz \quad . \tag{72}$$

If the substitutions

$$\delta u_1 = -\delta q_1 - \delta q_2 \sin \frac{\pi z}{\ell} \quad , \tag{73}$$

and

$$\delta u_2 = -\delta q_3 \sin \frac{2\pi z}{\ell} \quad , \tag{74}$$

53

are made and the integration over the length carried out
we have

$$\delta W_p = - [\delta q_1, \delta q_2, \delta q_3]
\begin{bmatrix}
m & \dfrac{2m}{\pi} & 0 \\[2mm]
\dfrac{2m}{\pi} & \dfrac{m}{2} & 0 \\[2mm]
0 & 0 & \dfrac{3m}{16}
\end{bmatrix}
\begin{bmatrix}
\ddot{q}_1 \\[1mm]
\ddot{q}_2 \\[1mm]
\ddot{q}_3
\end{bmatrix}
\quad , \qquad (75)$$

where $m = \rho \pi a^2 \ell$ (the displaced mass). The added mass matrix
is

$$[M_A] =
\begin{bmatrix}
m & \dfrac{2m}{\pi} & 0 \\[2mm]
\dfrac{2m}{\pi} & \dfrac{m}{2} & 0 \\[2mm]
0 & 0 & \dfrac{3m}{16}
\end{bmatrix}
\quad . \qquad (76)$$

B. STRUCTURAL MASS MATRIX

For a shell having mass μ per unit circumferential length
the kinetic energy in an axial length dz is taken to be

$$T_s{}' = \frac{1}{2}\, dz \int_0^{2\pi} \mu(\dot{u}^2 + \dot{v}^2)\, a\, d\theta \quad . \qquad (77)$$

But, from equations (58) and (59),

$$\dot{u} = \dot{u}_1 \cos\theta + \dot{u}_2 \cos 2\theta \quad , \qquad (78)$$

and $\qquad \dot{v} = -\dot{u}_1 \sin\theta - \frac{1}{2}\dot{u}_2 \sin 2\theta \quad , \qquad (79)$

54

where, from equations (62) and (63),

$$\dot{u}_1 = -\dot{q}_1 - \dot{q}_2 \sin \frac{\pi z}{\ell} \quad , \tag{80}$$

$$\dot{u}_2 = -\dot{q}_3 \sin^2 \frac{\pi z}{\ell} \quad . \tag{81}$$

Making the appropriate substitutions and evaluating the resulting integrals over θ and the length gives

$$2T_s = m_s \dot{q}_1^2 + \frac{4}{\pi} m_s \dot{q}_1 \dot{q}_2 + \frac{m_s}{2} \dot{q}_2^2 + \frac{3}{8} m_s \dot{q}_3^2 \quad , \tag{82}$$

where $m_s = 2\pi\mu a\ell$

= shell mass (including stiffening rings).

Adding the bulkhead mass m_b to the rigid body mode and including the added-mass-matrix the total kinetic energy becomes

$$2T = (m + m_s + m_b) \dot{q}_1^2 + \frac{4}{\pi} (m + m_s) \dot{q}_1 \dot{q}_2$$

$$\tag{83}$$

$$+ \frac{1}{2} (m + m_s) \dot{q}_2^2 + \frac{1}{64} (12m + 15m_s) \dot{q}_3^2 \quad .$$

For neutral buoyancy: $m = m_s + m_b$. Let $\beta = \frac{m_s}{m}$, then equation (83) can be written as

$$2T = \{\dot{q}\}^T [M] \{\dot{q}\} \quad , \tag{84}$$

55

where

$$[M] = m \begin{bmatrix} 2 & \frac{2}{\pi}(1+\beta) & 0 \\ \frac{2}{\pi}(1+\beta) & \frac{1}{2}(1+\beta) & 0 \\ 0 & 0 & \frac{1}{64}(12+15\beta) \end{bmatrix} . \qquad (85)$$

C. STRUCTURAL STIFFNESS MATRIX

The coefficients of the structural stiffness matrix are determined from energy considerations. The strain energy V is expressed in the form

$$2V = \{q\}^T [K]\{q\} . \qquad (86)$$

Since there is no strain energy associated with the rigid body mode and the other modes are elastically uncoupled, the stiffness matrix takes the form

$$[K] = \begin{bmatrix} 0 & 0 & 0 \\ 0 & k_{22} & 0 \\ 0 & 0 & k_{33} \end{bmatrix} . \qquad (87)$$

1. Shear Beam Mode

The modal displacements are given by equations (59). There is no ring bending and shell bending contributions are negligible, so that only membrane energy need be considered, i.e., $\varepsilon_\theta = 0$, $\varepsilon_z = 0$ and

56

$$\gamma_{z\theta} = \frac{\partial v}{\partial z} + \frac{1}{r}\frac{\partial w}{\partial \theta} = \frac{\pi}{\ell} q_3 \sin\theta \cos\frac{\pi z}{\ell} \quad . \tag{88}$$

The strain energy V_{sb} associated with the shear beam mode is given by

$$2V_{sb} = \int_0^\ell \int_0^{2\pi} G \, \gamma_{z\theta}^2 \, h_s \, a \, d\theta dz \quad , \tag{89}$$

or

$$2V_{sb} = \frac{G \, h_s \, a \, \pi^3}{2\ell} q_2^2 \quad . \tag{90}$$

2. Buckling Mode

The strain energy of the buckling mode is determined in two parts: the shell bending energy V_b and the membrane energy V_m. The modal displacements are given by equations (60).

The shell bending energy is given by

$$2V_b = \int_0^\ell \int_0^{2\pi} (D_z \kappa_z^2 + 2\nu D_z \kappa_z \kappa_\theta + D_\theta \kappa_\theta^2 + 4D_{z\theta}\kappa_{\theta z}^2) \, h_s a \, d\theta dz \quad , \tag{91}$$

where D_z and D_θ are the flexural rigidities given as

$$D_z = \frac{E h_s^3}{(12(1-\nu^2)} \quad , \tag{92}$$

and

$$D_\theta = \alpha \, D_z \quad . \tag{93}$$

57

The value α is a constant of proportionality determined by considering the orthotropic properties of the ring reinforced structure. The quantity $D_{\theta z}$ is the 'twisting' rigidity given by

$$D_{\theta z} = \frac{1 - \nu}{2} D_z \quad , \qquad \qquad \text{. (94)}$$

where effects of ring twisting are neglected.

The curvatures κ_z, κ_θ and $\kappa_{z\theta}$ are determined from equations (60) as:

$$\kappa_z = \frac{\partial^2 u}{\partial z^2} \quad , \qquad \qquad \kappa_\theta = \frac{1}{a^2} [\frac{\partial^2 u}{\partial \theta^2} + u] \quad ,$$

and

$$\kappa_{\theta z} = \frac{1}{a} \frac{\partial^2 u}{\partial \theta \partial z} \quad .$$

(95)

Substituting and performing the indicated integrations yields

$$2V_b = \frac{\pi D_z}{a^2} [2\pi^4 \frac{a^3}{\ell^3} + \frac{27}{8} \alpha \frac{\ell}{a} + 4(1 - \nu)\pi^2 \frac{a}{\ell} + \frac{3\nu\pi a}{\ell}] q_3^2 \quad .$$

(96)

The membrane energy is

$$2V_m = \int_0^\ell \int_0^{2\pi} (E'\epsilon_z^2 + G\gamma_{z\theta}^2) h_s a \, d\theta dz \quad , \qquad (97)$$

58

where

$$\varepsilon_z = \frac{\partial w}{\partial z} = \frac{2\pi\lambda}{\ell} q_3 \cos \frac{2\pi z}{\ell} \cos 2\theta \quad , \tag{98}$$

$$\gamma_{z\theta} = \frac{\partial v}{\partial z} + \frac{1}{r} \frac{\partial w}{\partial \theta} = q_3 \left(- \frac{\pi}{2\ell} - \frac{2\lambda}{a}\right) \sin \frac{2\pi z}{\ell} \sin 2\theta \quad , \tag{99}$$

$$E' = E/(1 - \nu^2) \quad .$$

Performing the indicated substitutions and evaluating the integrals gives

$$2V_m = \frac{\pi a \ell h_s}{2} \left[\frac{4\pi^2 \lambda^2}{\ell^2} E' + \left(\frac{\pi}{2\ell} + \frac{2\lambda}{a} \right)^2 G \right] q_3^2 \quad . \tag{100}$$

The parameter λ is determined by minimizing the membrane energy with respect to λ, i.e., $\frac{\partial V_m}{\partial \lambda} = 0$. The result of this minimization is

$$\lambda = \frac{-\pi \frac{\ell}{a}}{4\left(\pi^2 \frac{E'}{G} + \frac{\ell^2}{a^2}\right)} \quad . \tag{101}$$

The required coefficients of the stiffness matrix [K] are determined from equations (90), (96), (100) and (101).

D.   GENERALIZED FORCES

The generalized force vector {f} is determined by employing the virtual work principle. Let δW be the work done by the pressure p during a virtual displacement δq. Then

59

$$\delta W = - \int_0^{2\pi} \int_0^{\ell} p \left(\frac{\partial u}{\partial q_1} \delta q_1 + \frac{\partial u}{\partial q_2} \delta q_2 + \frac{\partial u}{\partial q_3} \delta q_3 \right) a \, dz d\theta \quad (102)$$

where $\frac{\partial u}{\partial q_1}$, $\frac{\partial u}{\partial q_2}$ and $\frac{\partial u}{\partial q_3}$ are determined from the modal displacement equations (58-60), i.e., $- \frac{\partial u}{\partial q_1} = \cos \theta$,

$- \frac{\partial u}{\partial q_2} = \sin \frac{\pi z}{\ell} \cos \theta$, $\quad - \frac{\partial u}{\partial q_3} = \sin^2 \frac{\pi z}{\ell} \cos 2\theta$. Evaluating

the integral over the surface

$$\delta W = [\delta q_1, \delta q_2, \delta q_3] \begin{bmatrix} f_1 \\ f_2 \\ f_3 \end{bmatrix}, \quad (103)$$

where

$$f_1 = a\ell \int_0^{2\pi} p \cos \theta \, d\theta \quad , \quad (104)$$

$$f_2 = \frac{2a\ell}{\pi} \int_0^{2\pi} p \cos \theta \, d\theta \quad , \quad (105)$$

$$f_3 = \frac{a\ell}{2} \int_0^{2\pi} p \cos 2\theta \, d\theta \quad . \quad (106)$$

The generalized forces are calculated from the two-dimensional finite element pressure-time history. The resulting generalized forces are given in Fig. 14. The rigid body force f_1 is in close agreement with the results calculated by Sette [1] and Murray [3] for a step pulse.
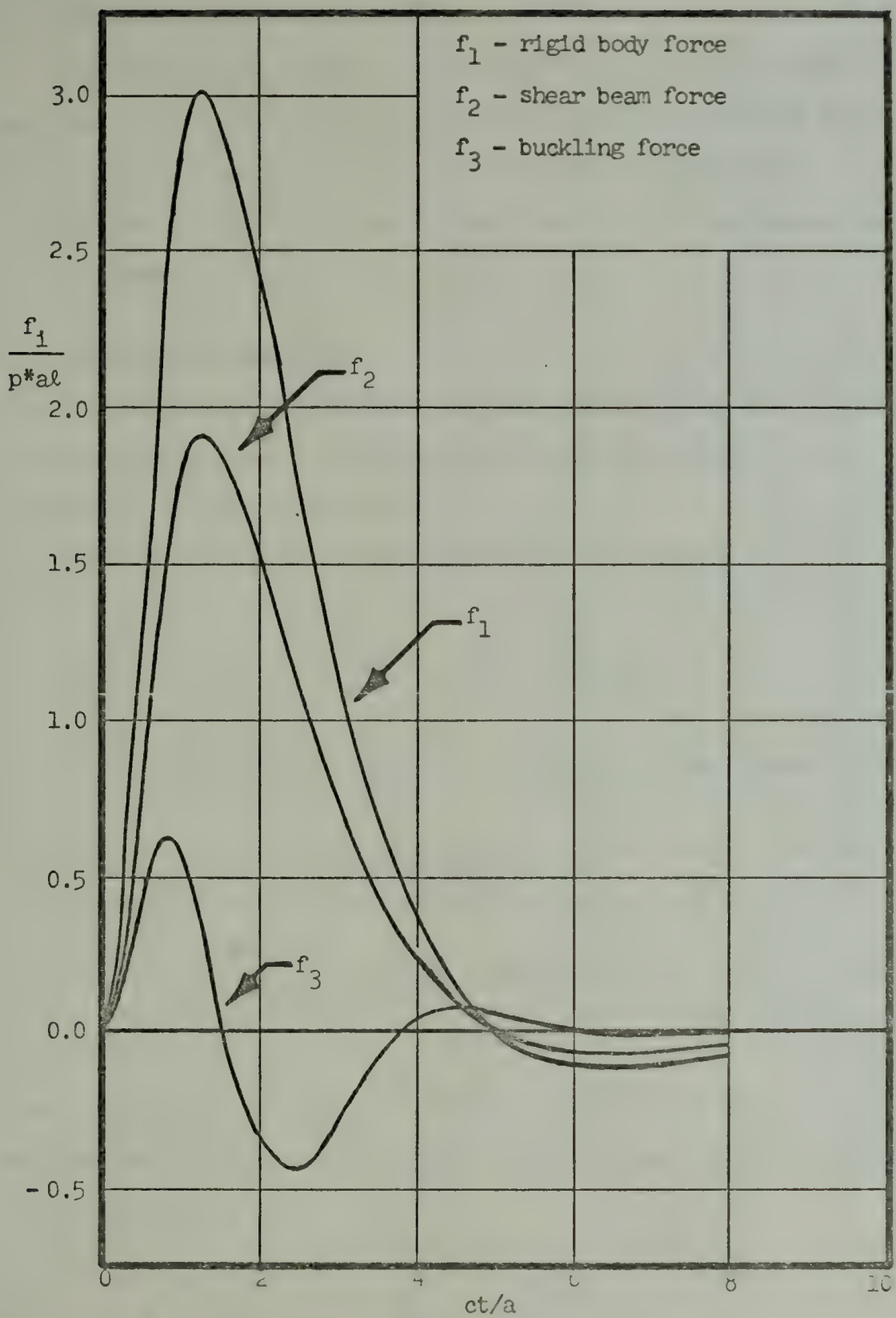
60

Fig. 14.   Generalized Forces-vs.-Time

E. GENERALIZED DISPLACEMENTS

The Newmark-β method, equation (42), of time integration was employed to evaluate the time dependent response of the structure. Figure 15 shows the resulting generalized displacements $(q_1 E/p^*a)$ as a function of the nondimensional time parameter ct/a.

F. STRUCTURAL STRESSES

The structural stresses are determined from the strain relations utilized to determine the coefficients of the structural stiffness matrix.

For the shear beam mode equation (88) gives

$$S_1 = \tau_{z\theta} = G\gamma_{z\theta} = G \frac{\pi}{\ell} q_3 \sin \theta \cos \frac{\pi z}{\ell} \quad . \tag{107}$$

For the buckling mode the stress due to ring bending is

$$S_2 = \sigma_\theta = Ec_1\kappa_\theta = Ec_1 \frac{1}{a^2} [\frac{\partial^2 u}{\partial r^2} + u]$$

$$= \frac{3Ec_1}{a^2} q_3 \sin^2 \frac{\pi z}{\ell} \cos 2\theta \quad , \tag{108}$$

where c_1 is the distance from the centroid of the cross-section to the extreme fiber. The membrane tension stress (equation (98)) is

$$S_3 = \sigma_z = E'\epsilon_z = 2E' \frac{\pi\lambda}{\ell} q_3 \cos \frac{2\pi z}{\ell} \cos 2\theta \quad , \tag{109}$$
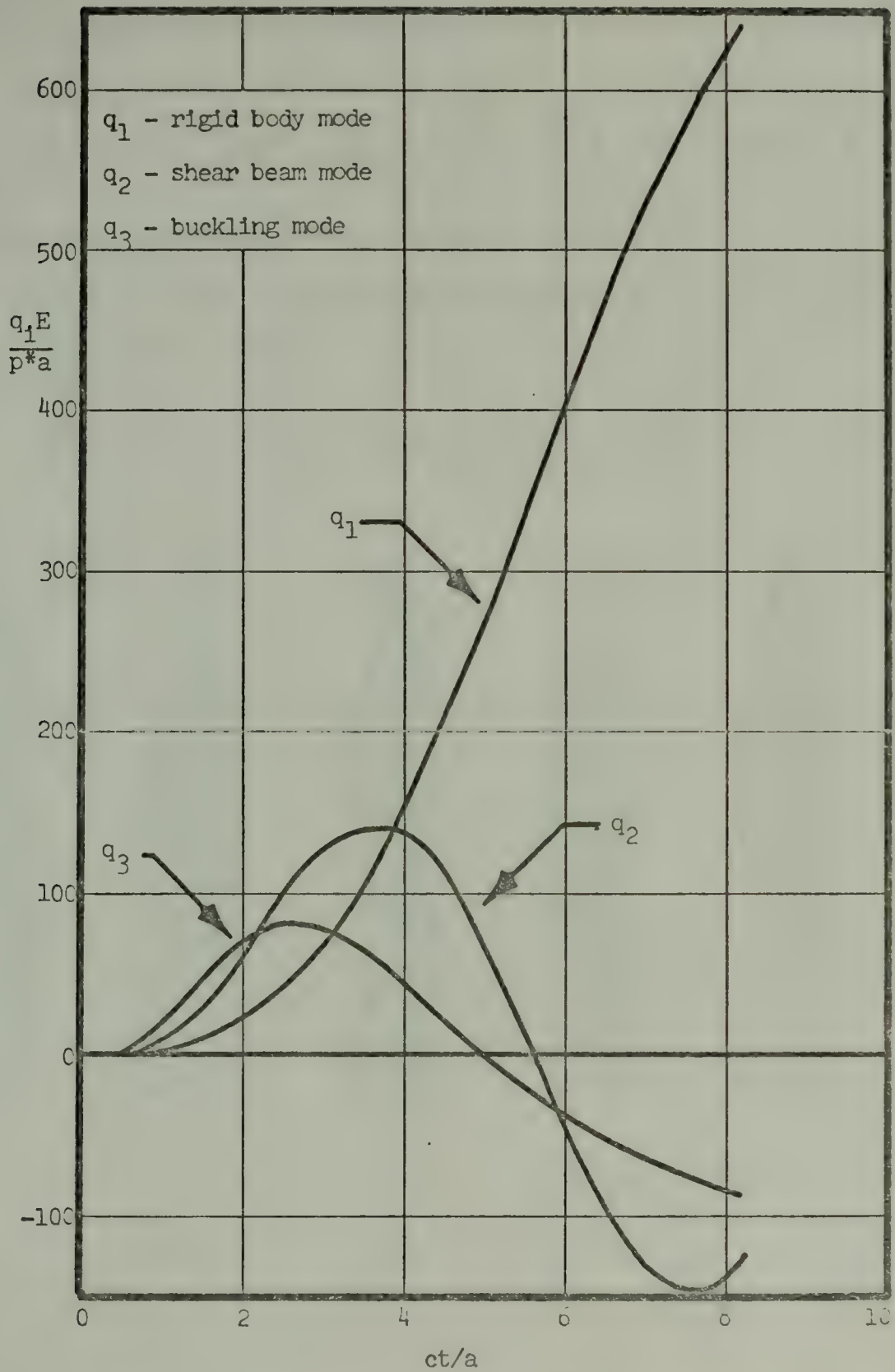
62

Fig. 15. Generalized Displacements-vs.-Time

and the membrane stress (equation (99) is

$$S_4 = \tau_{z\theta} = G\gamma_{z\theta} = G\,q_3\left(-\frac{\pi}{2\ell} - \frac{2\lambda}{a}\right)\sin\frac{\pi z}{\ell}\sin 2\theta\ , \quad (110)$$

where λ is determined from equation (101).

Table I shows the maximum nondimensional stresses S_1/p^* as a function of ct/a.

TABLE I.   MAXIMUM MODAL STRESSES

$\dfrac{ct}{a}$	$\dfrac{S_1}{p^*}$	$\dfrac{S_2}{p^*}$	$\dfrac{S_3}{p^*}$	$\dfrac{S_4}{p^*}$
0.33	0.049	0.035	-0.036	0.042
0.67	0.720	0.467	-0.469	0.553
1.00	3.242	1.880	-1.887	2.223
1.33	8.561	4.370	-4.386	5.167
1.67	16.644	7.351	-7.377	8.691
2.00	26.700	10.042	-10.078	11.873
2.33	37.616	11.897	-11.939	14.066
2.67	48.133	12.666	-12.711	14.975
3.00	56.972	12.354	-12.398	14.606
3.33	63.022	11.166	-11.206	13.202
3.67	65.468	9.399	-9.433	11.112
4.00	63.825	7.325	-7.351	8.660
4.33	57.947	5.143	-5.161	6.080
4.67	48.057	2.978	-2.989	3.521
5.00	34.732	0.893	-0.896	1.056
5.33	18.850	-1.095	1.099	-1.295
5.67	1.511	-2.987	2.998	-3.531
6.00	-16.046	-4.783	4.800	-5.654
6.33	-32.544	-6.479	6.502	-7.660
6.67	-46.772	-8.063	8.092	-9.534
7.00	-57.680	-9.510	9.544	-11.244
7.33	-64.455	-10.788	10.826	-12.755
7.67	-66.585	-11.863	11.906	-14.026
8.00	-63.895	-12.709	12.754	-15.026

V.   CONCLUSIONS AND RECOMMENDATIONS

The results of this investigation confirm that the finite element method provides a satisfactory numerical method of evaluating the interaction of a plane acoustic blast wave and a rigid structure. Extension of the method to other two and three-dimensional geometries using the techniques employed appears to be practical.

The submarine structural model is a simple three degree-of-freedom model. It was chosen to provide an illustrative example of the implementation of the superposition theorem and not as a general model of a submarine.

It is recognized that a more sophisticated model is necessary to determine the response of a submarine subjected to blast wave loading. To improve the model it would be advantageous to:

a.   Include additional modes, particularly a 'breathing' mode to incorporate the effects of hydrostatic loading;
b.   Distribute and elastically mount the mass of the sub-marine not included in the shell;
c.   Remove the restrictions on the rigidity of the bulkheads.

Incorporating the above improvements and nonlinear structural characteristic into the submarine model will provide for a more complete analysis of the dynamic response of a submarine to blast-wave loading.

APPENDIX A

PRESSURE-vs.-TIME AT THE RIGID CYLINDER-FLUID INTERFACE FOR θ = 30°, 60°, 90°, 120° and 150°

The pressure-time histories at the rigid cylinder-fluid interface at θ = 30°, 60°, 90°, 120° and 150° are shown in Figs. 16-20. The solid line represents Sette's [1] results displaced along the time axis to coincide with the incidence of the constant portion of the cubic ramp-step wave. Sette [1] provided no data for θ = 120° and θ = 150° and therefore no comparison is available. Data for θ = 0° and θ = 180° is presented in Figs. 9 and 10.

The integration, wave and mesh characteristics are:

$$\frac{ch}{a} = \frac{1}{6} \quad ,$$

$$\frac{c\tau_r}{a} = 0.97 \quad ,$$
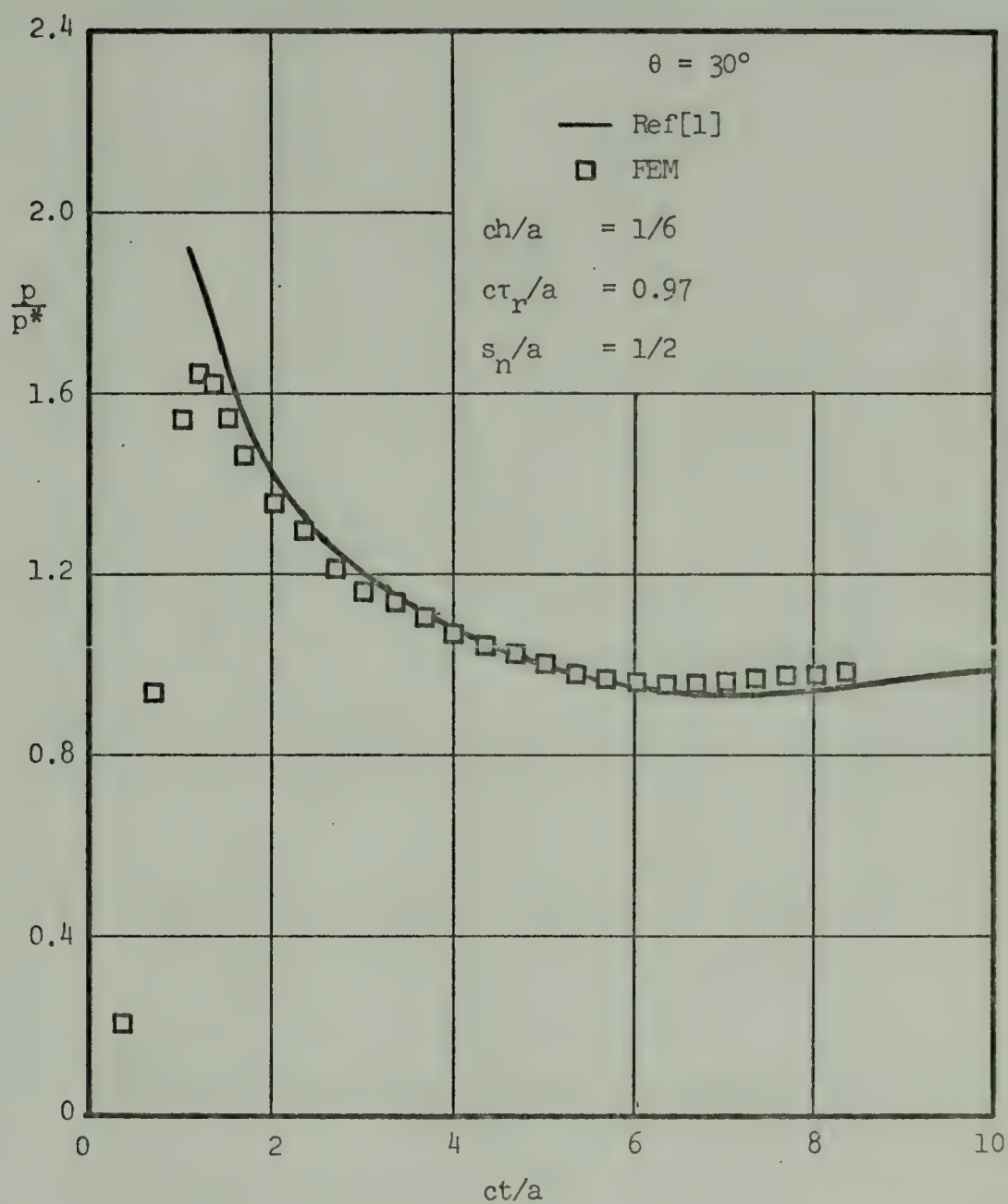
$$\frac{s_n}{a} = \frac{1}{2} \quad .$$

Fig. 16. Pressure-vs.-Time at the Rigid Cylinder-
Fluid Interface ($\theta = 30°$)

Fig. 17. Pressure-vs.-Time at the Rigid Cylinder-Fluid Interface ($\theta = 60°$)

68

Fig. 18. Pressure-vs.-Time at the Rigid Cylinder-
Fluid Interface ($\theta = 90°$)
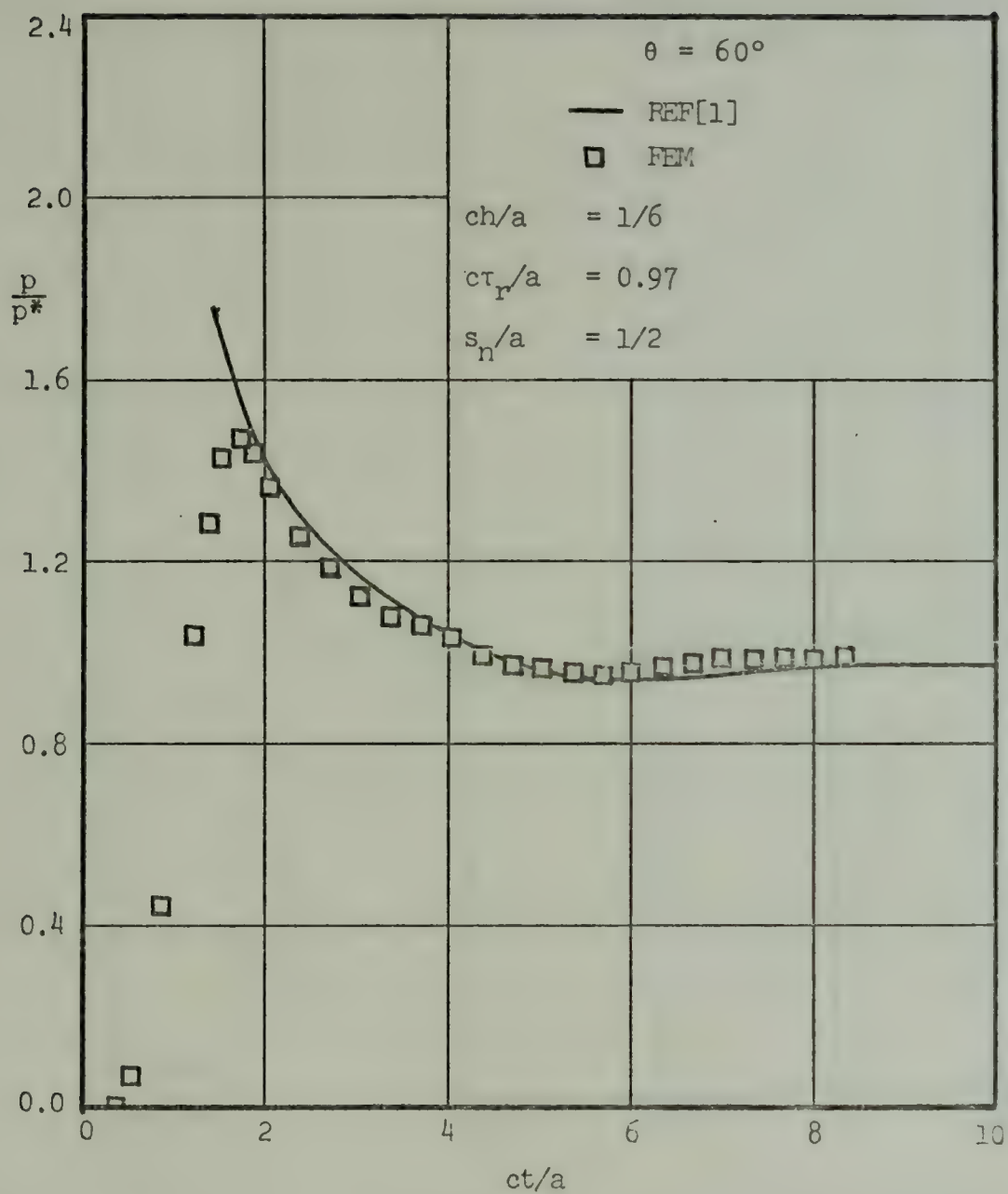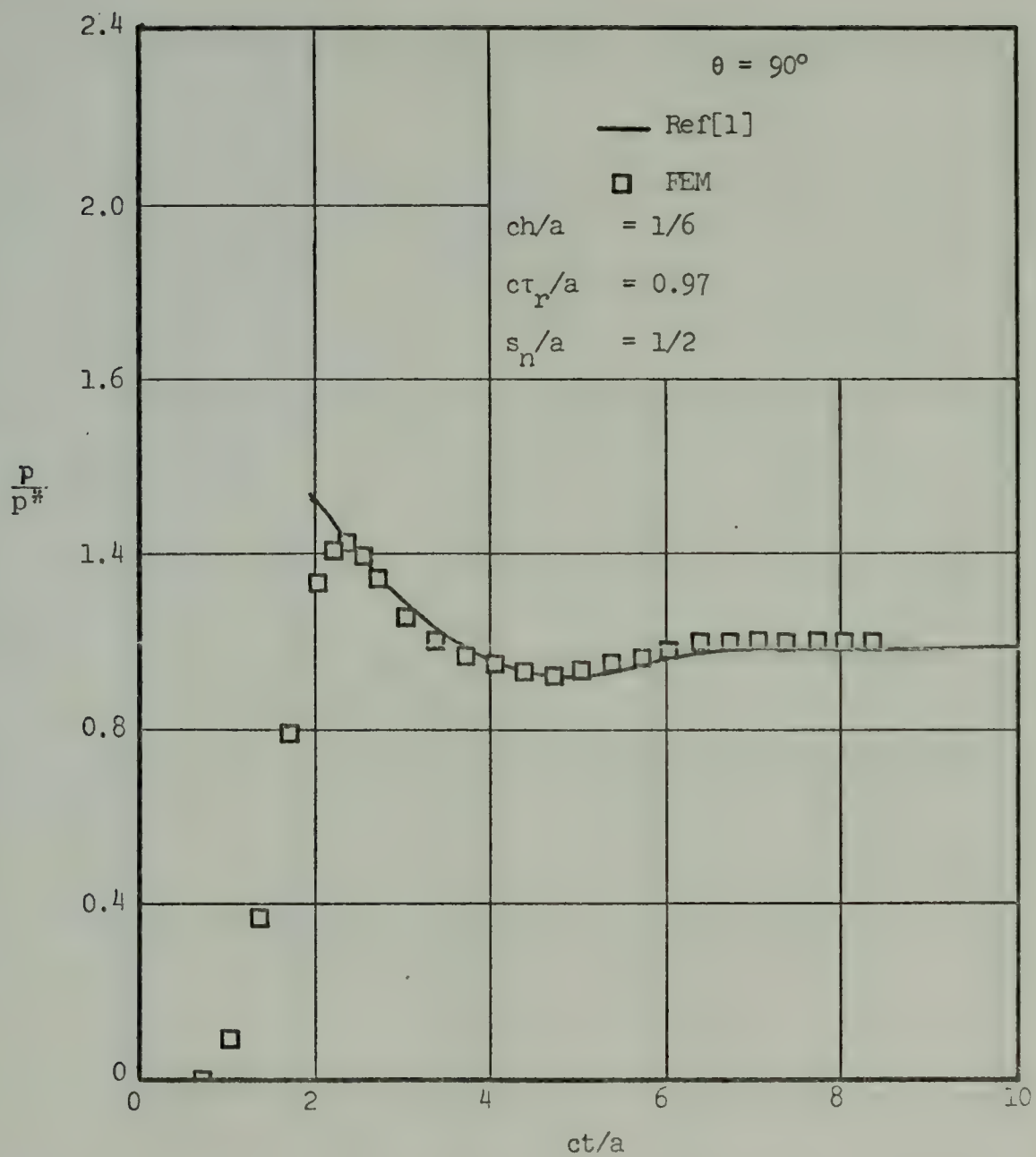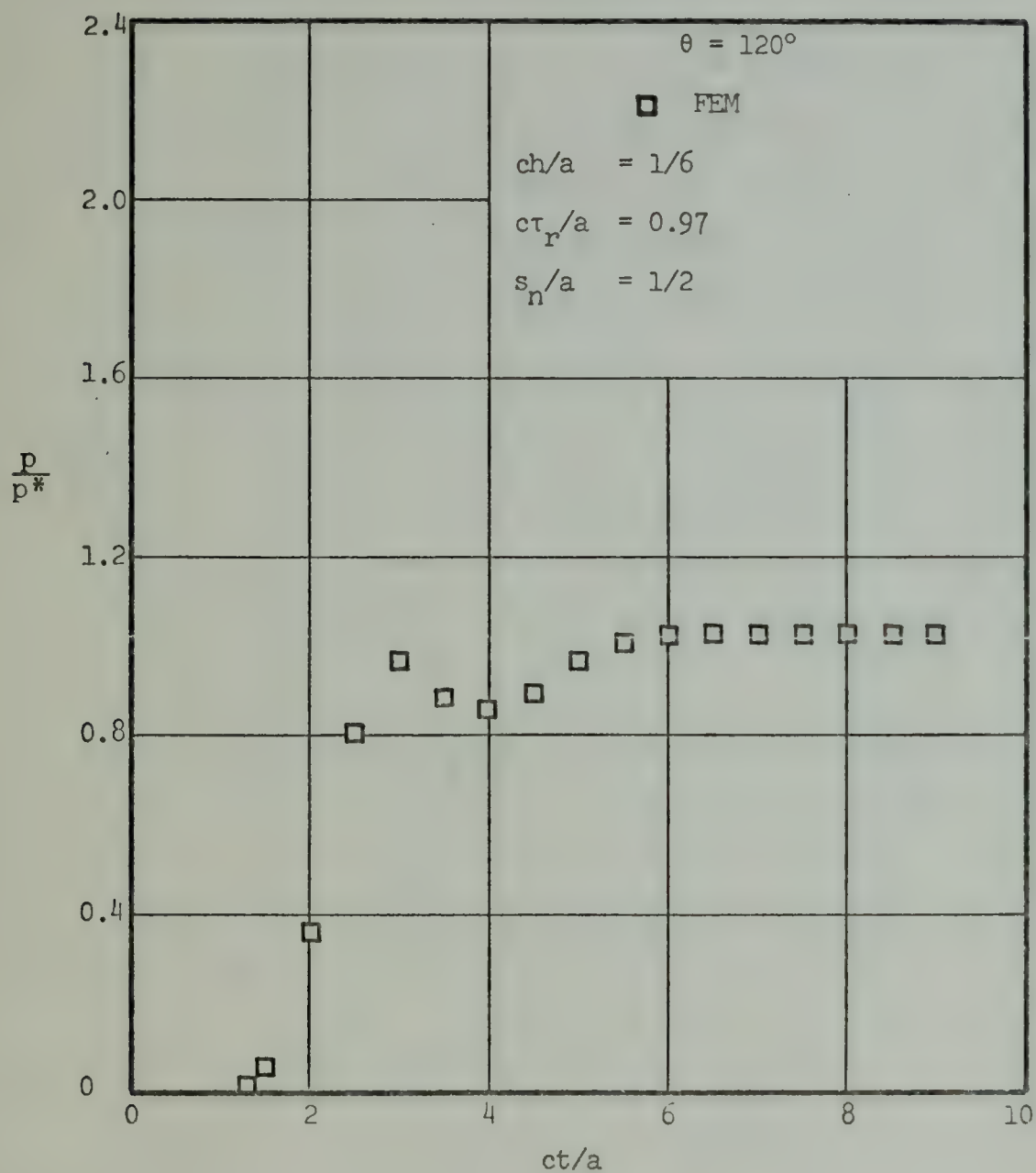
Fig. 19.   Pressure-vs.-Time at the Rigid Cylinder-
           Fluid Interface ($\theta = 120°$)
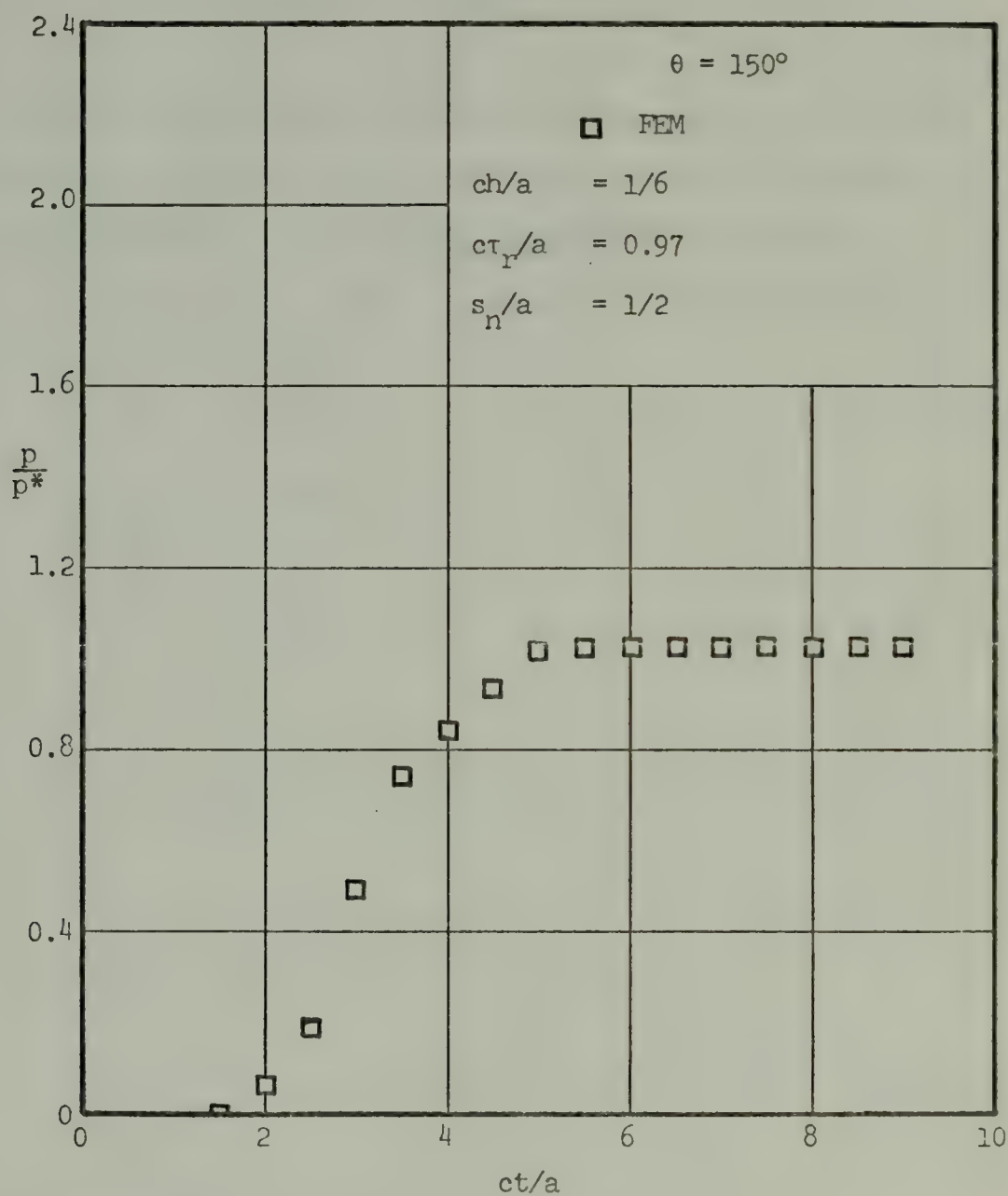
Fig. 20. Pressure-vs.-Time at the Rigid Cylinder-Fluid Interface ($\theta = 150°$)

APPENDIX B

TABULATED PRESSURE-TIME HISTORY
AT THE RIGID CYLINDER-FLUID INTERFACE

The following tabulated data is the result of a two-dimensional finite element solution of the interaction of a ramp-step wave and a rigid cylindrical structure.

The integration, wave and mesh characteristics are:

$$h = a/6c,$$

$$\tau_r = 0.97\ a/c,$$

$$s_n = \frac{1}{2}\ a\ .$$

p/p* AT INDICATED ANGLE AND TIME

ct/a / θ°	1/3	2/3	1	1 1/3	1 2/3	2	2 1/3	2 2/3	3
0.5	0.50	1.32	1.71	1.61	1.45	1.39	1.32	1.24	1.19
7.5	0.48	1.30	1.71	1.62	1.45	1.38	1.32	1.24	1.19
15.0	0.42	1.23	1.69	1.63	1.46	1.38	1.32	1.24	1.19
22.5	0.34	1.12	1.64	1.64	1.47	1.38	1.31	1.23	1.18
30.0	0.23	0.95	1.56	1.64	1.48	1.37	1.30	1.23	1.18
37.5	0.14	0.77	1.44	1.63	1.50	1.37	1.30	1.22	1.17
45.0	0.08	0.56	1.24	1.58	1.51	1.38	1.29	1.21	1.16
52.5	0.03	0.37	1.03	1.49	1.52	1.39	1.28	1.20	1.15
60.0	0.02	0.23	0.77	1.31	1.49	1.40	1.28	1.19	1.14
67.5	0.01	0.12	0.53	1.10	1.41	1.37	1.28	1.18	1.13
75.0	0.01	0.07	0.34	0.89	1.25	1.30	1.24	1.17	1.11
82.5	0.00	0.03	0.19	0.59	1.06	1.15	1.18	1.16	1.09
90.0	0.00	0.02	0.10	0.32	0.82	0.98	1.03	1.14	1.07
97.5	0.00	0.01	0.05	0.13	0.58	0.76	0.87	1.09	1.06
105.0	0.00	0.00	0.03	0.06	0.39	0.54	0.67	1.05	1.05
112.5	0.00	0.00	0.01	0.03	0.22	0.36	0.47	0.75	1.03
120.0	0.00	0.00	0.00	0.01	0.13	0.21	0.32	0.58	0.97
127.5	0.00	0.00	0.00	0.00	0.06	0.13	0.12	0.41	0.90
135.0	0.00	0.00	0.00	0.00	0.03	0.06	0.06	0.28	0.78
142.5	0.00	0.00	0.00	0.00	0.01	0.03	0.03	0.17	0.64
150.0	0.00	0.00	0.00	0.00	0.01	0.02	0.02	0.11	0.50
157.5	0.00	0.00	0.00	0.00	0.00	0.01	0.02	0.07	0.36
165.0	0.00	0.00	0.00	0.00	0.00	0.00		0.06	0.27
172.5	0.00	0.00	0.00	0.00	0.00	0.00			0.20
180.0	0.00	0.00	0.00	0.00	0.00	0.00			0.18

TABLE II. PRESSURE AT THE RIGID CYLINDER-FLUID INTERFACE

p/p* AT INDICATED ANGLE AND TIME

θ°	3⅓	3⅔	4	4⅓	4⅔	5	5⅓	5⅔	6
0	1.16	1.14	1.10	1.07	1.05	1.03	1.01	0.99	0.98
7.5	1.16	1.14	1.10	1.07	1.05	1.03	1.01	0.99	0.98
15.0	1.16	1.14	1.10	1.07	1.05	1.03	1.01	0.99	0.98
22.5	1.16	1.13	1.09	1.07	1.04	1.02	1.01	0.99	0.98
30.0	1.15	1.13	1.09	1.06	1.04	1.01	1.00	0.98	0.98
37.5	1.15	1.12	1.08	1.05	1.03	1.01	0.99	0.98	0.98
45.0	1.13	1.12	1.07	1.04	1.02	1.00	0.99	0.98	0.98
52.5	1.12	1.10	1.06	1.03	1.01	0.99	0.98	0.98	0.98
60.0	1.10	1.08	1.05	1.02	0.99	0.98	0.98	0.97	0.98
67.5	1.08	1.06	1.04	1.00	0.98	0.97	0.97	0.98	0.99
75.0	1.07	1.04	1.02	0.99	0.97	0.96	0.97	0.98	1.00
82.5	1.04	1.02	1.00	0.97	0.96	0.95	0.97	0.98	1.01
90.0	1.02	0.99	0.97	0.95	0.95	0.95	0.98	0.99	1.02
97.5	0.99	0.96	0.94	0.94	0.94	0.96	0.99	1.00	1.03
105.0	0.97	0.93	0.92	0.92	0.93	0.97	0.99	1.01	1.03
112.5	0.95	0.90	0.89	0.90	0.93	0.99	1.00	1.02	1.03
120.0	0.93	0.87	0.86	0.97	0.93	1.00	1.03	1.03	1.03
127.5	0.90	0.85	0.84	0.87	0.94	1.02	1.03	1.03	1.03
135.0	0.85	0.83	0.83	0.88	0.96	0.99	1.04	1.04	1.03
142.5	0.78	0.82	0.84	0.89	0.98	1.00	1.04	1.03	1.03
150.0	0.68	0.78	0.87	0.94	1.00	1.02	1.03	1.04	1.04
157.5	0.58	0.75	0.89	0.98	1.01	1.03	1.03	1.03	1.04
165.0	0.49	0.72	0.90	1.00	1.03	1.02	1.02	1.03	1.04
172.5	0.44	0.68	0.90	1.01	1.03	1.02	1.03	1.03	1.04
180.0	0.40	0.63	0.91	1.02	1.03	1.02	1.02	1.03	1.04

TABLE II. PRESSURE AT THE RIGID CYLINDER—FLUID INTERFACE (continued)

p/p* AT INDICATED ANGLE AND TIME

$\theta°$ \ ct/a	$6\frac{1}{3}$	$6\frac{2}{3}$	7	$7\frac{1}{3}$	$7\frac{2}{3}$	8
0.0	0.97	0.97	0.97	0.97	0.98	0.99
7.5	0.97	0.97	0.97	0.97	0.98	0.99
15.0	0.97	0.97	0.97	0.98	0.99	1.00
22.5	0.97	0.97	0.97	0.98	0.99	1.00
30.0	0.97	0.98	0.98	0.99	0.99	1.00
37.5	0.98	0.98	0.98	0.99	1.00	1.00
45.0	0.98	0.98	0.99	1.00	1.00	1.00
52.5	0.99	0.99	1.00	1.00	1.01	1.00
60.0	0.99	1.00	1.00	1.01	1.01	1.01
67.5	1.00	1.01	1.01	1.01	1.01	1.01
75.0	1.01	1.01	1.02	1.02	1.02	1.02
82.5	1.02	1.02	1.02	1.02	1.02	1.02
90.0	1.03	1.03	1.02	1.03	1.03	1.03
97.5	1.03	1.03	1.03	1.03	1.03	1.03
105.0	1.03	1.03	1.03	1.04	1.04	1.03
112.5	1.03	1.04	1.04	1.04	1.04	1.04
120.0	1.03	1.04	1.04	1.04	1.04	1.04
127.5	1.04	1.04	1.04	1.04	1.04	1.04
135.0	1.04	1.04	1.05	1.04	1.04	1.04
142.5	1.04	1.04	1.05	1.05	1.05	1.04
150.0	1.04	1.04	1.05	1.05	1.05	1.04
157.5	1.04	1.05	1.05	1.05	1.05	1.04
165.0	1.04	1.05	1.05	1.05	1.05	1.04
172.5	1.04	1.05	1.05	1.05	1.05	1.04
180.0	1.04	1.05	1.05	1.05	1.05	1.04

TABLE II. PRESSURE AT THE RIGID CYLINDER-FLUID INTERFACE (concluded)

APPENDIX C

SUBMARINE STRUCTURAL PARAMETERS

The specific structural parameters used in the calculation of the coefficients of equation (57) are:

ρ = fluid density = 9.36×10^{-5} lbf sec^2/in^4

E = 30×10^6 psi,

G = 11.6×10^6 psi,

ν = 0.300,

a = hull radius = 180 in.,

ℓ = bulkhead spacing = 480 in.,

h_s = shell thickness = 1.60 in.,

β = m_s/m = 0.200

The internal ring reinforcing frames are characterized by:

Frame spacing = 36.1 in.,

Web thickness = 1.10 in.,

Frame depth = 9.20 in.,

Flange width = 9.20 in.,

Flange thickness = 1.80 in.,

α = orthotropic constant of proportionality = 127.

The mass matrix is

$$[M] = \begin{bmatrix} 9.405 & 3.592 & 0. \\ 3.592 & 2.821 & 0. \\ 0. & 0. & 1.102 \end{bmatrix} \times 10^3 \text{ lbf sec}^2/\text{in.}$$

The stiffness matrix is

$$[K] = \begin{bmatrix} 0. & 0. & 0. \\ 0. & 107.9 & 0. \\ 0. & 0. & 2.236 \end{bmatrix} \times 10^6 \text{ lbf/in.}$$

LIST OF REFERENCES

1. Sette, W.J., <u>Pressure Produced on a Non-Yielding Cylinder by a Step-Pulse</u>. Washington D.C.: Catholic University of America Press, 1951.

2. Mindlin, R.D., and H.H. Bleich, "Response of an Elastic Cylindrical Shell to a Transverse Step Shock Wave." <u>J. Appl. Mech.</u>, Vol. 20, No. 2 (June, 1952), 189-195.

3. Murray, W.W., "Interaction of a Spherical Acoustic Wave With a Beam of Circular Cross Section." Underwater Explosions Research Division Report 1-55, Norfolk Naval Shipyard, 1955.

4. Bleich, H.H., "Dynamic Interaction Between Structures and Fluid." In <u>Structural Mechanics</u>, edited by J.N. Goodier and N.J. Hoff. New York: Pergamon Press, 1960. Pp. 263-284.

5. Berglund, J.W. and J.N. Klosner, "Interaction of a Ring Reinforced Shell and a Fluid Medium." <u>J. Appl. Mech.</u>, Vol. 35, No. 1 (March, 1968), 139-147.

6. Zienkiewicz, O.C., B.M. Irons and B. Nath, "Natural Frequencies of Complex Free or Submerged Structures by the Finite Element Method." <u>Proc. Conf. Vibrations</u> Civil Eng., London: Butterworths, 1965, Pp. 83-93.

7. Zienkiewicz, O.C. and R.E. Newton, "Coupled Vibrations of a Structure Submerged in a Compressible Fluid." In <u>Finite Element Techniques</u>, edited by M. Sörensen. Stuttgart, Germany: University of Stuttgart, Pp. 359-380.

8. Zienkiewicz, O.C., <u>The Finite Element Method in Engineering Science</u>. New York: McGraw-Hill, 1971.

9. Nath, Bhaskar, "Dynamics of Structure-Fluid Systems." In <u>Advances in Hydroscience</u>, Vol. 9, edited by Ven Te Chow, New York: Academic Press, 1973. Pp. 85-118.

10. Chan, S.P., H.L. Cox and W.A. Benfield, "Transient Analysis of Forced Vibrations of Complex Structural-Mechanical Systems." <u>J. Royal Aero. Soc.</u>, Vol. 66 (July, 1966), 457-460.

11. Houbolt, John C., "A Recurrence Matrix Solution for the Dynamic Response of Elastic Aircraft." <u>J. Aero. Sci.</u>, Vol. 17, No. 9, (Sept., 1950), 540-550.

12. Newmark, Nathan M., "A Method of Computation for
     Structural Dynamics." <u>J. Eng. Mech.</u>, Vol. 66 (July,
     (1959), 67-96.

INITIAL DISTRIBUTION LIST

INITIAL DISTRIBUTION LIST

No. Copies

1. Defense Documentation Center
   Cameron Station
   Alexandria, Virginia 22314   2

2. Library, Code 0212
   Naval Postgraduate School
   Monterey, California 93940   2

3. Department Chairman, Code 59
   Department of Mechanical Engineering
   Naval Postgraduate School
   Monterey, California 93940   1

4. Professor U. S. Newton, Code 59Ne
   Department of Mechanical Engineering
   Naval Postgraduate School
   Monterey, California 93940   2

5. Lt. Donald L. Atchison, USN
   14708 Power Mesa Drive
   Poway, California 92064   1

6. Naval Ship Research and Development Center
   Design Applications Branch
   ATTN: Mr. L. Mann Gilford Jr. (Code 1735)
   Bethesda, Maryland 20034   1

7. Naval Ship Systems Command (SHIPS 03)
   Washington, D.C.   1

8. Professor C.L. Harrison, Code 60Hs
   Department of Mechanical Engineering
   Naval Postgraduate School
   Monterey, California 93940   1